Jouni Mykkänen

Delineation of Brain Structures from Functional Positron Emission Tomography Images

ACADEMIC DISSERTATION

To be presented, with the permission of the Faculty of Information Sciences of the University of Tampere, for public discussion in the Paavo Koli Auditorium of the University on July 4th, 2003, at 12 noon.

DEPARTMENT OF COMPUTER AND INFORMATION SCIENCES
UNIVERSITY OF TAMPERE

A-2003-2
TAMPERE 2003

Supervisor: Professor Martti Juhola
Department of Computer and Information Sciences
University of Tampere

Opponent: Professor Jussi Parkkinen
Department of Computer Science
University of Joensuu

Reviewers: Professor Jyrki Kuikka
Faculty of Medicine, Clinical Physiology
University of Kuopio

Professor Ari Visa
Signal Processing Laboratory
Tampere University of Technology

Department of Computer and Information Sciences
FIN-33014 UNIVERSITY OF TAMPERE
Finland

ISBN 951-44-5712-9
ISSN 1457-2060

Electronic dissertation

Acta Electronica Universitatis Tamperensi 271
ISBN 951-44-5724-2
ISSN 1456-954X
http://acta.uta.fi

Tampereen yliopistopaino Oy
Tampere 2003

Abstract

Positron emission tomography (PET) imaging is a unique method for studying biochemical processes involved in living species. It provides quantitative information about the processes at a cellular level, which is needed, for example in diagnosis of a disease and the development of new drugs. Quantitative information can be determined from PET images by extracting volumes of interest. In order to collect large databases of the functional data derived from PET, new automatic methods for image analysis are required. The delineation of PET images is a challenging task due to noise and individual data contents in PET images. It has not gained attention that it deserves.

This study proposes a new lossless image compression method and novel approaches to delineate brain surfaces from PET brain images. First, a low complexity lossless image compression method was developed for noisy PET brain images. Next, a user-guided software using intensity values of image was developed and utilized to determine quantitative values from the PET brain images. Next, a two-dimensional deformable model and the corresponding anatomical references from MR images were applied to delineate cortical surfaces from PET brain images. Deformable models are advanced delineation methods entailing geometric shape and evolution rules, which connect the model to data providing its adaptation to the salient features in an image. This method was able to improve the registration alignment and correct differences between the anatomical and functional structures. However, proper segmentation of volumetric PET images required a new three-dimensional deformable surface model which was developed in close collaboration with this study. It uses a global optimization to avoid the initialization problem common with deformable models. The new method was applied to extract surfaces from images in PET brain studies with ^{18}FDG and ^{11}C-Raclopride radiopharmaceuticals. The delineation procedure was fully automatic, repeatable and considerably faster than the entirely manual delineation methods applied with PET images. Consequently, the coarse cortical structures for the hemispheres were determined in an iterative way and no anatomical references or user interactions were required in the process.

This study contributes novel approaches for semi-automatic and fully auto-

matic surface delineation from PET brain images. In addition, an image compression procedure for PET brain images is proposed. These provide new possibilities for developing fully automatic applications for neurological image analysis and databases.

Key words brain surface extraction, volume of interest, deformable model, three-dimensional image analysis, mid-sagittal plane, segmentation, compression

Preface

This work was carried out in the Department of Computer Science and Applied Mathematics, University of Kuopio, 1997, and the Department of Computer and Information Sciences, University of Tampere during the years 1998-2003. This work was accomplished in collaboration with the Tampere University of Technology and Turku PET Centre.

I wish to express my sincere gratitude to my supervisor Docent Ulla Ruotsalainen Ph.D., who introduced me to the fields of positron emission tomography imaging, modeling, and scientific thinking. Her scientific advice as well the countless discussions with her has made this thesis possible.

I express my sincere thanks also to my other supervisor, Professor Martti Juhola, Ph.D., who suggested the topic of present study, and for all kinds of support during the preparation of this thesis.

I am greatly indebted to my co-author, Jussi Tohka, MSc., who continuously expanded our understanding of deformable models. I also express my special thanks to co-author Timo Tossavainen MSc., for inspiring discussions, and to co-authors Sakari Alenius Ph.D., and Jouni Luoma MSc.

I express my deep gratitude to my reviewers, Professors Jyrki Kuikka and Ari Visa. Their valuable comments and advice clarified many details of the manuscript.

I want to express my sincerest thanks to the other members of the Methods and Models for Biological Signals and Images (M^2oBSI) group and the staff of Turku PET Centre for their skillful support. I also want to thank to my colleagues in the department as well as elsewhere.

I thank my very good friends for giving me time and attention when I have needed them.

I want to express my thanks to my parents Esko and Irja, and to my sister Miia for their support and understanding.

This work was financially supported by the Tampere Graduate School in Information Science and Engineering (TISE), the Foundation of Instrumentarium, the Jenny and Antti Wihuri Foundation, the Oskar Öflund Foundation, which are all gratefully acknowledged.

Tampere, 23rd June 2003

Jouni Mykkänen

Contents

Symbols and Abbreviations

symbol or abbreviation.	explanation	first referenced or defined
λ	regularisation parameter	29
AC	anteriour commisure, a landmark in brain	13
AIR	automatic image registration	18
AMIR	automatic multi-modality image registration	18
ET	emission tomography	2
CT	computerized (computed) tomography	1
DM-DSM	deformable model and dual surface minimization	42
DPCM	differential pulse code modulation	47
DSM-OS	deformable model, outer surface modification	42
FBP	filtered back projection	7
FDG	fluoro-2-deoxy-D-glucose	5
FDOPA	fluoro-dopaminium	37
fMRI	functional magnetic resonance imaging	2
FOV	field of view	4
FWHM	full width at half maximum	4
the grid	network-based computing infrastructure	21

symbol or abbreviation.	explanation	first referenced or defined
ICBM	The International Consortium for Brain Mapping	14
ML	maximum likelihood	7
MLEM	maximum likelihood expectation maximization	7
MNI	The Montreal Neurological Institute	14
MR	magnetic resonance	1
MRP	median root prior	8
PC	posteriour commisure, a landmark in brain	13
PET	positron emission tomography	3
PVE	partial volume effect	10
ROI	region of interest	41
SPECT	single-photon emission computerized tomography	2
SPET	single-photon emission tomography	2
SPM	statistical parametric mapping	18
T&T	Talairach and Tourneux brain atlas	12
VOI	volume of interest	40
VRML	virtual reality modelling language	44

List of Publications

I. J. Mykkänen, T. Tossavainen and M. Juhola. Lossless compression of emission tomography images. In A. Hasman, Blobel B., J. Dudeck, R. Engelbrecht, G. Gell, and H.-U. Prokosch, editors, *Medical Infobahn for Europe, Proceedings of MIE2000 and GMDS2000*, pages 1240–1244, IOS Press, 2000.

II. J. Mykkänen, M. Juhola and U. Ruotsalainen. Extracting VOIs from brain PET images. *International Journal of Medical Informatics*, 58–59(1):51–57, 2000.

III. J. Mykkänen, J. Tohka and U. Ruotsalainen. Automated delineation of brain structures with snakes in PET. *In Physiological Imaging of the Brain with PET*, pages 39–43, Academic Press, 2000.

IV. U. Ruotsalainen, J. Mykkänen, J. Luoma, J. Tohka and S. Alenius. Methods to improve repeatability in quantification of brain PET images. In F. Rattay, editor, *World Congress on Neuroinformatics*, ARGESIM Report 20, pages 659–664, ARGESIM/ASIM Verlag Vienna, 2001.

V. J. Mykkänen, J. Tohka and U. Ruotsalainen. Delineation of brain structures from emission tomography images with deformable models. In R. Baud, M. Fieschi, P. Le Beaux and P. Ruch, editors, *The New Navigators: from Professionals to Patients*, volume 95, pages 33-38, IOS Press, 2003.

VI. J. Mykkänen, J. Tohka, J. Luoma and U. Ruotsalainen. Automatic extraction of brain surface and mid-sagittal plane from PET images applying deformable models. Technical Report, A-2003-1. Department of Computer

and Information Sciences, University of Tampere, 2003.
(http://www.cs.uta.fi/reports/r2003.html)

Chapter 1

Introduction

IMAGING is the methodology and technology which together provide data acquisition and its representation as an image form. The last century produced several imaging methodologies suitable for measuring biological structures and their functions. These are known as medical imaging. The technological development in recent decades has seen medical imaging widely applied all over the world, opening up completely new possibilities to expand our knowledge about living species and to apply it on a regular basis to disease diagnostics. Unfortunately, the development has led to information explosion and, consequently, difficulties to control, to classify, and to analyze the collected data. New advanced models and methodologies are needed to accomplish these tasks properly.

The objective of medical imaging is to provide quantitative and qualitative information on species for purposes of research and medical decision-making. Medical imaging includes the measurement, reconstruction, analysis, and representation of biological structures and processes as images. This is a challenge for the computational methods applied. The information on images can be examined qualitatively and quantitatively. Medical imaging is divided into structural and functional imaging methods. Structural imaging aims to measure and to represent the anatomical structures of the object. Such imaging methods are magnetic resonance (MR) imaging and computed tomography (CT) X-ray imaging [Hor03, KS01]. Both of they are suitable for studying living (in vivo) and dead (in vitro) species. Functional imaging can provide information about the biochemical processes occurring in a subject over time, and is a useful method for studying

living species. Functional magnetic resonance imaging (fMRI) [FMR03] and emission tomography (ET) are such methods. Emission tomography includes single photon emission computed tomography (SPECT), also known as single photon emission tomography (SPET), and positron emission tomography (PET) imaging methods [UCL03]. There are also other methods available for structural as well as functional imaging, but they are beyond the scope of this study, which set focus on PET imaging.

Positron emission tomography provides quantitative information about the studied function which allows comparison of different individuals. This makes it possible to detect abnormalities present in functionality before the actual symptoms of a disease are visible and to follow its current stage in detail. Quantification of cellular level functions also plays an important role in drug development in the medical industry. However, extracting quantitative values from images is not a straightforward operation. The image resolution and signal-to-noise ratio are relatively low compared to the structural images. The complex data acquisition and image reconstruction processes require advanced hardware as well as computational methods, which may be difficult to control. The properties of the studied function may be highly individual, particularly in the case of the neurological structures.

Quantification of functions from PET brain images can be performed by extracting the structures. Due to the nature of function and the properties of PET images, automatic and accurate structure extraction is rarely possible. Structure extraction is usually performed by manually drawing regions on image cross-sections and using some low-level segmentation tools. With a large set of images, possibly delineated by several clinicians, robust and accurate structure extraction is a rather demanding and laborious task. For the automatic quantification of functional images, the structure extraction method should be automatic. This could improve the accuracy of the quantification of structures.

The objectives of the present study is to explore computational structure extraction and related topics with PET brain images. The main interest is to find a general and automatic procedure for delineating brain surfaces from PET images.

Chapter 2

Functional Positron Emission Tomography

2.1 Introduction to Positron Emission Tomography Imaging

POSITRON emission tomography (PET) is based on a radio-labeled biologically active compound, tracer, its detecting and a model. The model describes the kinetics of the tracer as it is involved in a biological process. The process can be measured by registering the radiation emitted by the tracer and calculating the tracer concentration. The final result is represented as a three-dimensional image. Repeating the scan, a tissue function can be followed over time. An overview example of PET technique is represented in Figure 2.1. A good introduction to PET can be found in [UCL03], see also [KS01, Chapter 4.2.3] and [Bro95, Chapter 69].

All tissue functions are based on biochemical processes involved in cells. For example, blood flow, membrane transport, metabolism and ligand-receptor interactions are such processes. The physiological effect of processes can be studied with PET imaging. The determination of biochemical functions is a complex multidisciplinary task entailing data acquisition, image reconstruction, and image analysis steps. Data acquisition in functional imaging requires advanced technical equipment and trained staff. In addition, emission tomography methods require

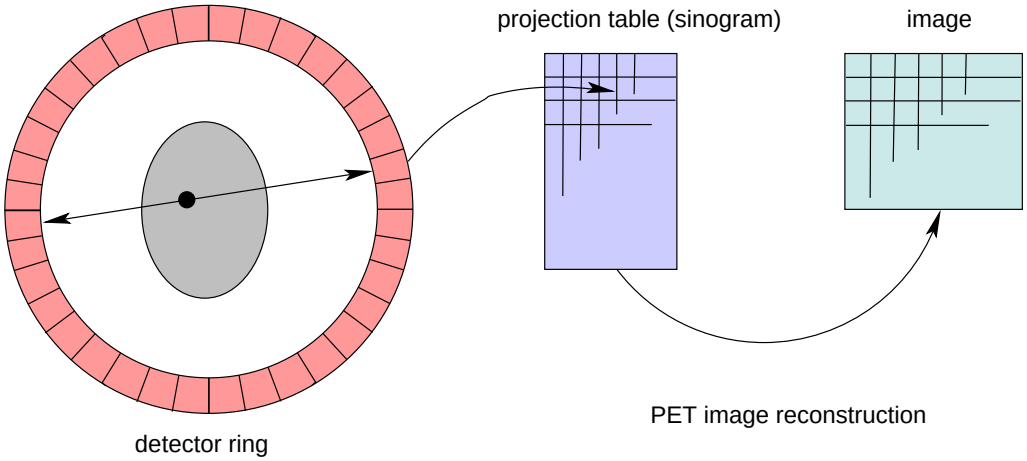

Figure 2.1: Overview of positron emission tomography imaging. Data acquisition and image reconstruction process for a single count is shown. A pair of photons is registered as a count and stored into the sinogram. The image is reconstructed from the sinogram.

a cyclotron unit for the required radio-isotope production. Image reconstruction and analysis need good models and methods to extract information properly from acquired data.

2.1.1 Acquisition Techniques for PET

In PET, a tracer includes an unstable nucleus which emits photons when being transformed into a stable isotope. Photons are registered around the subject with detectors which are positioned on a ring or detectors circulate around the object. The registered photons are called counts. The counts are collected in a sinogram, which is a two-dimensional table representing all projections. The field of view (FOV) is the area inside detector ring where the counts can be registered. The resolution of a PET scanner is defined as a full width at half maximum (FWHM) distribution of a measured count.

In positron emission tomography, a released positron from an unstable nucleus and an electron annihilate into two photons. The photons travel in almost opposing directions. Registering the coincidence of two photons, a line where annihilation

took place can be determined (Figure 2.1.) The acquired coincides, counts, are stored in a sinogram. The radiation is specific for the applied radiopharmaceutical. It originates only from the tracer administrated to species allowing exact quantification of radioactivity concentration. This is a unique feature of PET.

The data acquisition process has several noise sources. Radioactive decay is a random process, but with a large number of nucleus, it follows statistical Poisson distribution. A released positron may travel a significant distance from the nucleus before meeting an electron. Thus, the location of annihilation cannot be defined precisely. In practice, the spatial resolution is limited to about three millimeters [Bud95], [Ruo97, Chapter 2.2]. The spatial resolution of the collected data is affected by scattering, accidental coincidence, variance in sensitivity of individual detectors, and size and number of detectors.

2.1.2 Quantification in PET

Positron emission tomography provides a way to measure and quantify biochemical processes. However, complicated natural systems are fairly difficult to model properly with insufficient measurements and limited knowledge. An excessively complex but insufficient model can easily lead to problems caused by the model itself. It is better to keep the model of the system as simple as possible.

The compartment model is a simplified mathematical model for anatomical and physiological systems [Ruo97, Chapter2.3]. The system under study can be modelled by dividing it into separate blocks. The radioactive compounds exchange between the blocks, and can accumulate in the cells. The accumulated concentration of the tracer can be measured by the PET scanner. The two-block model consists of the blood plasma and the cell blocks are shown in Figure 2.2 (a). The cell block can be divided into two parts, exchange and uptake. The three-block model is shown in Figure 2.2 (b). The same models can also be applied to the single photon emission tomography (SPET).

The pharmaceutical matters applied in positron emission tomography to label compounds are ^{11}C, ^{13}N, ^{15}O, and ^{18}F. If possible, they should be connected to the normal molecules involved in biochemical processes. FDG (fluoro-2-deoxy-D-glucose) is the most used tracer in positron emission tomography, because the

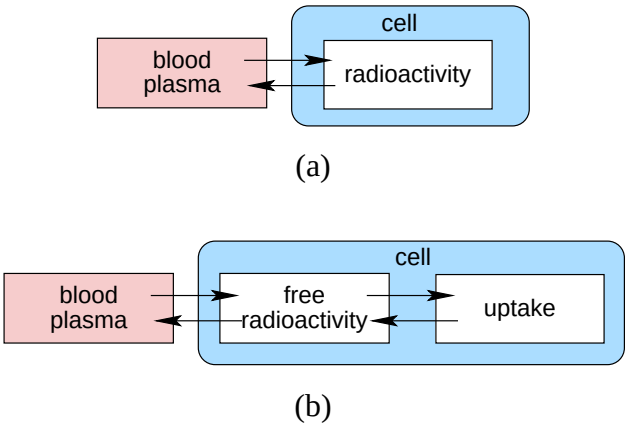

Figure 2.2: Description model of metabolic radioactivity. a) A two-block model and b) a three-block model.

radioactivity concentrates on the tissue studied and does not return to the blood plasma.

The compartment model can be applied with a reference region approach [GLHC97, AKK+99]. The image itself is used to derive the input for the method instead of using the blood samples. For example, the block models can be applied with two separate tissues, the target and reference areas. The reference area is such that it has similar properties to the structure under study, except that the radioactivity does not concentrate on the reference tissue. That property can be utilized to solve the actual uptake concentration from the target area. The two-block model is applied to the reference area and the three-block model to the target.

It is possible and preferable to transfer image analysis operations to the projection space and perform calculations straight from sinogram data for accurate quantification. For example, this approach was utilized in the study [KTJ+97]. The structures extracted from the corresponding MR images were transferred to the observation space of the PET scanner for quantification of function.

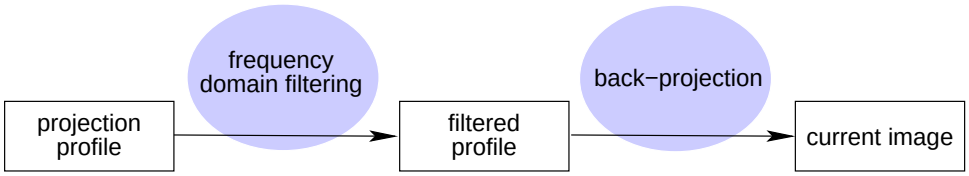

Figure 2.3: Filtered back-projection for a single projection profile. The profile is projected back over the image at a given angle. The process is repeated for each profile in the sinogram.

2.2 Image Reconstruction Methods for PET

The reconstruction from data to image is traditionally modelled by Radon transform [Rus95, Chapter 9]. Reconstructing the image from its projections (sinogram) is to compute the inverse Radon transform. This is an ill-posed inverse problem. One common solution for PET is to use *the filtered back projection* (FBP) method, which was originally developed for the reconstruction of CT images [KS01, Chapter 3]. Each projection profile in the sinogram is transferred to the frequency space, filtered, and returned to the spatial space. The filtered projection is back-projected over the image at a given angle. The overview of FBP for a single projection is represented in Figure 2.3. The FBP method is sensitive to Poisson noise. The noise level can be reduced by filtering, but at the cost of lowered image resolution. This is not a desirable feature with PET.

Another possibility is to apply statistical iterative methods to the reconstruction problem. With an iterative method the algorithm compares the image to the measured data and improves the next iteration image so that the calculated projections have a better correlation to the measured sinogram.

Maximum likelihood (ML) is an iterative method for trying to find the best possible estimate[1] [Moh87, Chapter 3.8]. With the maximum likelihood expectation maximization (MLEM) method, an initial guess image is set for the first image. The current image is forward-projected to projections and compared to the original projections to determine the corrections for the next iteration. The MLEM algorithm overview is shown in Figure 2.4. However, the MLEM tends

[1] A unified formalism for the estimation theory can be found in [Kar97].

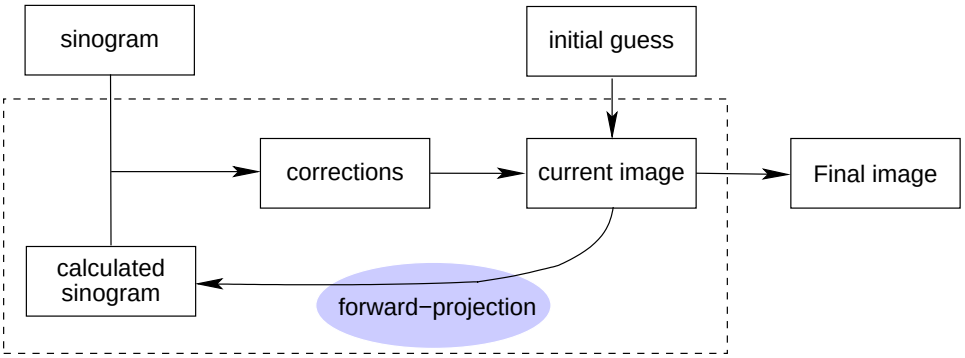

Figure 2.4: MLEM process overview. At the beginning, the initial estimate image is created. It is forward-projected to the projection space and compared to the original projections to determine corrections. Corrections are updated to the current image. The process is repeated until the current image meets the aimed quality criteria.

to increase the noise for each iteration. With Bayes methods, the prior default distribution for the image is utilized for the MLEM iteration to reduce noise. Applied prerequisites (priors) may include anatomic image, analytic energy function, and median root prior (MRP) [AR97, ARA98]. The MRP method assumes that the most probable value of the pixel is close to the local median of surrounding pixels.

Examples of FBP and MRP reconstructed images from the same FDG-PET brain study and the same measurement are shown in Figure 2.5 (a) and (b) respectively. The images are from the selected coronal, sagittal, and transaxial views, near the middle area of the brain.

2.3 Properties of PET Images

The properties of reconstructed positron emission tomography images originate from several sources in the imaging process [Bud95]. These can be divided into those originating from the subject, applied data acquisition technique and reconstruction method. In the image, the resolution and noise level are likely to be the most important properties setting physical limitations what can be extracted from an image. The resolution can be divided into spatial and time resolutions.

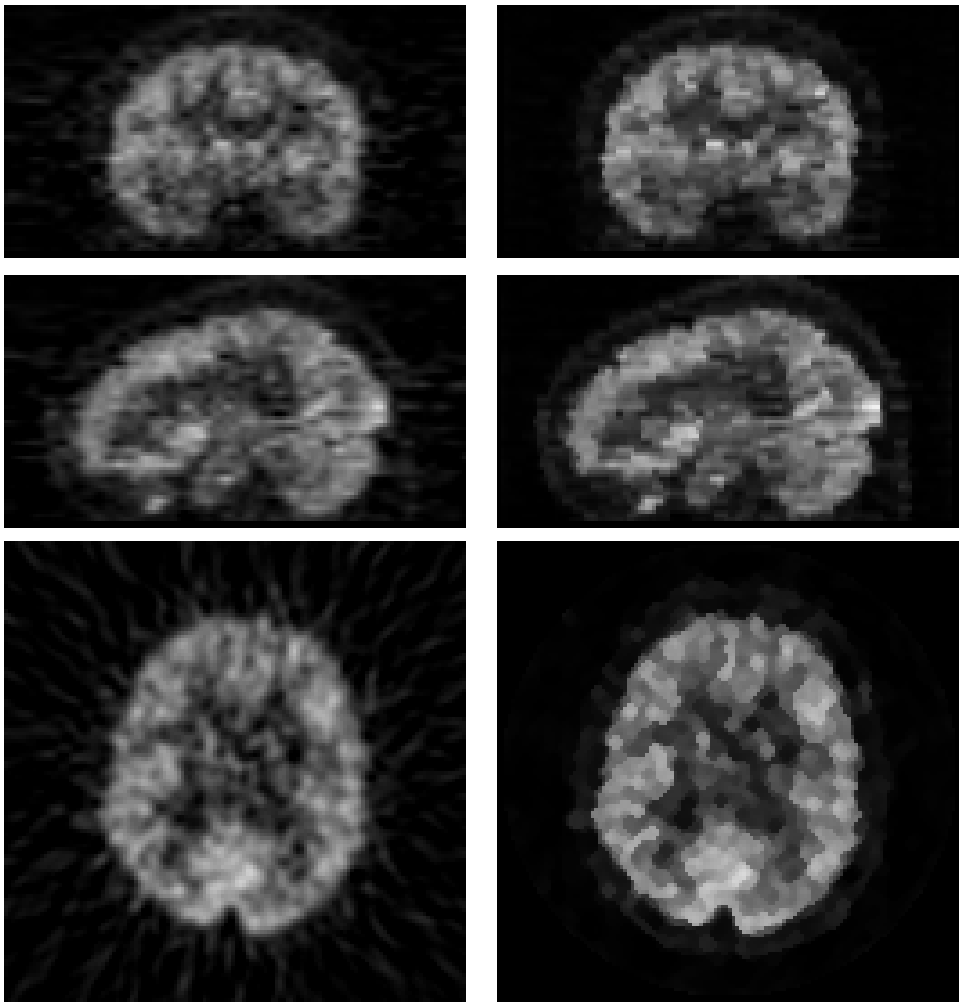

(a) (b)

Figure 2.5: A FDG-PET brain image reconstructed with (a) FBP method and (b) median root prior method. From top, transaxial, coronal and sagittal cross-section views.

Whereas the spatial resolution defines the smallest physical size for the target that can be recognized, the time resolution defines the smallest time period that it is possible to capture from a metabolic process. Both ultimately depend on the scanner hardware applied. However, the complex reconstruction process applied may significantly affect the spatial resolution and the noise level of a final image. For example, the conventional FBP method produces artifacts in the reconstructed images which can be seen around the target on the FBP reconstructed image in Figure 2.5 (a).

The size of a measured target may be smaller than the smallest measurable unit of a scanner. In *a partial volume effect* (PVE), a single voxel in an image includes data from several tissues. It produces systematic errors in estimated quantitative physiological parameters. In *a spill-over*, the higher radioactivity in target area spreads to the surrounding tissues. As a consequence, the surrounding tissues have a higher radioactivity concentration than they should have. This should be taken into account with accurate regional image analysis. These are delicate topics in functional imaging research at present waiting for proper solutions [Iid02].

Scanning a living species may pose several practical problems. To avoid unnecessary radiation dose, the amount of the pharmaceutical should be as low as possible to recognize the object. With many PET brain studies, the subject should be alert during the scan to follow a desired function. Any physical movements in the field of view cause distortions in the data collected during the scan. Depending on the study, scanning may take a long time, up to an hour, increasing the likelihood of movement. Emotional studies may cause unwanted reflexes. Illnesses may be difficult with respect to physical actions. The subject inside the field of view may be fixed to avoid physical movements. The head is normally fixed by some supporting material, however, it cannot fully prevent movements. Tighter fixing is inconvenient and may disturb the actual functional study.

To summarize, the properties of positron emission tomography images pose a real challenge for any attempts to analyze images in a robust, accurate and automatic way. The contrast, noise and resolution in images are the most important properties to be considered when developing new methods for analysing PET images.

Chapter 3

Computational Methods for Neurological Images

3.1 Atlases and Coordinate Systems for Brain Image Analysis

ALL human brains have the same main anatomical structures: cerebrum, cerebellum, and ventricles [Gra80, Chapter 7]. The brain is divided into the left and right hemispheres, which are connected. The cerebrum consists of grey matter and white matter structures. Grey matter or cortex is an outer part and it is an individually convoluted tissue, a few millimeters thick. Figure 3.1 represents the main structures of the human brain. These structures provide a guideline for neurological studies. The brain surface can be applied to identify the brain structure including all the sub-structures. For a brain study, the hemispheres need to be coarsely separated in a brain image. This can be done by determining the mid-sagittal plane of the brain. Automated approaches can be found in the literature based on cross-correlation of the intensity values between the hemispheres and the symmetry of brain boundaries [AKK97, LCR01].

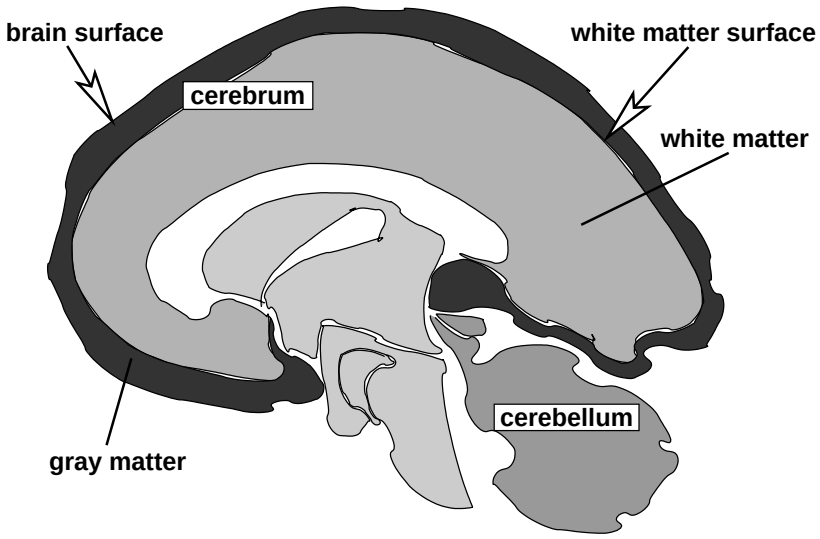

Figure 3.1: Mid-sagittal sketch of anatomical human brain structures. Cerebrum including grey matter and white matter tissues and cerebellum are represented.

3.1.1 Brain Atlases for Neurological Imaging

A brain atlas is a representative image, where the common anatomical structures of brain are represented. Brain mapping methods try to transform individual images into the atlas space to allow the direct comparison of images. Existing brain atlases are based on the anatomical structures of the brain. Structures are obtained from post mortem studies or magnetic resonance images. Some individual variances are removed from the atlas, because they could disturb brain mapping process.

The Talairach and Tourneax brain atlas and coordinate system

The Talairach and Tourneax (T&T) brain atlas is widely applied to brain image fusion and brain mapping [Tal88]. It is created on the basis of the sliced brain from a dead female adult. Due to individual nature of the brain structures, the use of one subject as a representative of others is not generally a good idea. Nevertheless, the Talairach and Tourneax proportional brain atlas is widely applied in brain mapping research. It was the first proper brain atlas commonly accepted for clinical use

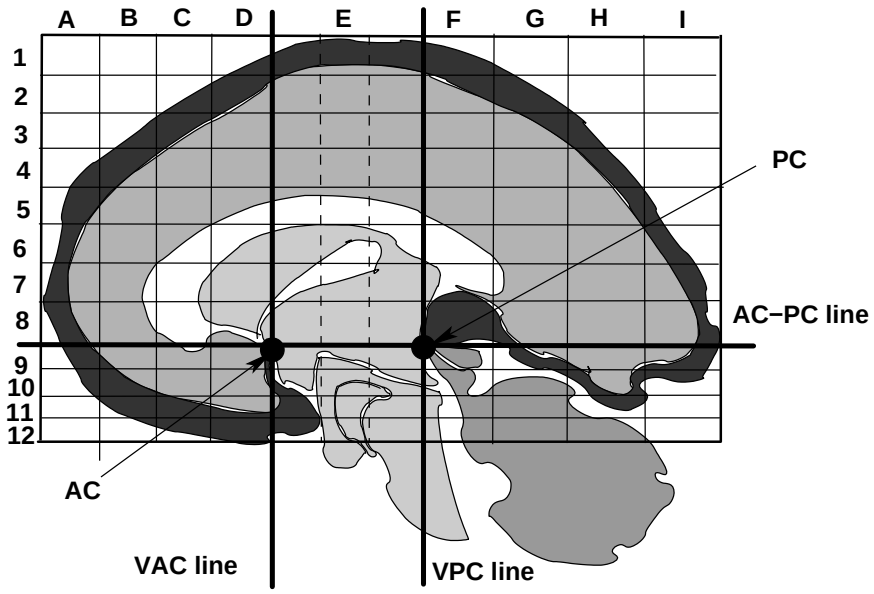

Figure 3.2: Proportional grid of the Talairach stereo-tactic coordinate system. The grid is overlayed over the earlier sketch (Figure 3.1), which was slightly rotated. The Talairach coordinate system is based on anteriour commisure (AC) and posterior commisure (PC).

and, hence it has attained a reference status.

Definitely the most important contribution of the work of Talairach and Tournaux is the underlying idea how an individual brain is mapped to the atlas. The T&T coordinate system is based on *the anteriour commisure* (AC) and *posteriour commisure* (PC) which exist in every normal subject's brain. These landmarks define three lines, the AC-PC line, the vertical anteriour commisure (VAC) line and the vertical posteriour commisure (VPC) line. From these baselines and the current outer surfaces, the brain is proportionally split to labelled areas. Figure 3.2 presents the landmarks, baselines, and the grid positioned on the previously introduced sketch in Figure 3.1. In the third dimension, the left and the right hemispheres are split similarly to get the full three-dimensional grid for the brain structure.

MNI brain atlases

The Montreal Neurological Institute (MNI) has created brain atlases which are more representative of the population than the Talairach and Tourneax atlas. The first MNI305 brain atlas was created from 305 normal magnetic resonance scans [ECM+93]. It was included in the SPM96 distribution [SPM03]. The newer ICBM152 atlas image is the average of 152 normal magnetic resonance scans. The scans have been matched to the MNI305 with the nine parameter affine transformations. It is the standard template in the SPM99 software package and International Consortium for Brain Mapping (ICBM) [SPM03, ICB03]. Unfortunately, the MNI atlas images slightly differ from the Talairach atlas image. The MNI atlases appear to be slightly larger than the Talairach atlas. This way cause inaccuracies of image analysis in MNI space if the MNI descriptions are not available. The Talairach descriptions are difficult to transform to the MNI space.

Applications for brain atlases

Brain atlases can be applied to segmentation, coregistration and labelling of new brain images. They provide relevant information about the structures to be identified from new images. For example, the Talairach proportional atlas is applied to extract brain structures from single photon emission tomography (SPET) images in the article [MDB+94]. The anatomic structure is delineated for regions of interest (ROIs) in the atlas and transferred to the image, which is set in the Talairach coordinate grid system.

The Talairach and Tourneaux atlas image with the coordinate system provides a map of the general brain structures. With the labels, this is an efficient tool for many problems arising in the field of brain mapping. However, complex structures, such as the cortex, require more precise description. Highly individual cortex might be better handled separately from the other brain structures. Brain atlases can be dedicated to a disease-specific purpose [TMT01].

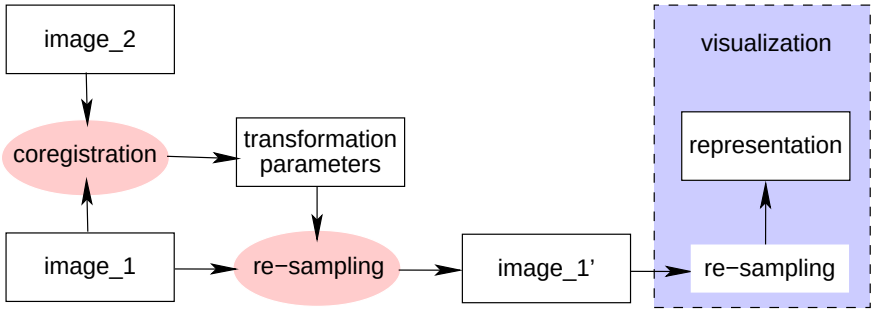

Figure 3.3: Overview of image fusion. At first, a mapping function between images (image_1 and image_2) is determined. This can be linear or non-linear function. Then, the image data (image_1) are transformed into the reference image space (image_1'). Image representation is the physical appearance of the image data on a display or printer. The images need to be re-sampled according to the output hardware.

3.2 Fusion of Neurological Images from Different Modalities

Brain images originating from different acquisition techniques need to be brought into the same spatial and intensity space. Differences in resolutions and intensities need to be removed in order to compare content of images. These differences are caused by the acquisition techniques themselves and different standards for handling and representing image data [KIMW00]. In fusion, conventionally, images originate from different imaging modalities for the same individual. Fusion can be divided into a coregistration and visualization of images. Visualization of images includes re-sampling and physical representation methods for images. Physical representation includes the methods for preparing the digital data for conversion into analog form, which may have several limitations such as limited contrast. Figure 3.3 gives an overview of image fusion.

Image coregistration, or registration, is a fundamental operation to find similarities between two images. With automatic approaches, image registration is formed as an optimization problem. Optimization is the act of obtaining the best result under given circumstances [Rao78, Page 1]. The aim is to minimize or maximize the desired property, which is formed as an objective function. It

provides a quantitative measure to compare the similarity of two images. A maximum of this similarity measure gives a solution for the registration problem. However, in general, a similarity measure is difficult to define and highly application dependent. Reviews of image registration can be found, for example, in [Bro92, MV98, HBTL02].

The coregistered images are brought to the same coordinate space by resampling the images applying the determined transformation parameters. Transformations can be divided into the rigid-body and non-rigid methods. A rigid-body transformation includes translations and three rotations for each dimension. Translations refers to the straight movements in coordinate space and rotations defines angles how to rotate data around the coordinate axis. A non-rigid transformation includes a rigid-body transformation as the first step. Scaling defines the changes in the size of the data for each dimension. Affine transformations include rotation, scaling, translation and shearing [PS85, Chapter 1].

The nine parameter rigid-body transformation can be formed as a matrix operation [FvDFH91, Chapter 5]. The right-handed coordinate system is often applied to matrices. The order of the multiple operations affects the final result and the special cases need to be taken into account.

3.3 Registration Methods for Neurological Images

Brain images are challenging for automatic image registration methods because of their highly individual structures and functions. Different acquisition techniques produce fundamentally different images, which may contain only little usable information for establishing a correspondence between images. In medical imaging, registration problems can be divided into four categories based on subject and modality [HBTL02]. The categories are represented in Table 3.1.

The overall idea to obtain a registration is to find appropriate transformation parameters for the image to be transformed into the reference image space. At first, initial parameters are selected and applied to the image. Then, the similarity function is calculated between the new image and the reference image. If it is not a maximum of the similarity, transformation parameters are updated for the next iteration. When the maximum for the similarity function is found, images are in

Table 3.1: Four types of image coregistration problems with subjects and scanning devices (modalities).

	modality	
subject	**intra**	**inter**
intra	images of the same subject acquired in the same modality	images of the same subject across different modalities
inter	images of different subjects in the same modality	images of different subjects across different modalities

coregister and the transformation parameters are determined for the image.

3.3.1 Registration Categories for Brain Images

Intra-subject, intra-modality

Alignment of brain studies in the same subject acquired in the same modality can be matched based on an extrinsic coregistration method. An extrinsic method relies on an external marker or references in the scanner space. It assumes that the distance between the markers is the same in both the images. With the same scanner and the same subject, this can be done accurately. In other cases, the image content needs to be considered by using an intrinsic method.

Intra-subject, inter-modality

Intrinsic methods can be divided into feature-based and voxel-based methods. Features are common geometric properties existing in images to be applied to determine a coregistration. A feature-based method may be based on landmarks or surfaces present in images. A landmark is the point that can be identified from both the images to be coregistered. A mapping between the images is determined based on the landmarks by minimizing a penalty function. For example, the least-squares fitting of two three-dimensional point sets is presented in [AHB87]. In practice, the number of landmarks is rather limited and the complete description

of a complex elastic mapping of brain images may not be feasible. However, manual landmark-based methods are widely applied in clinical practice because of their simplicity and easy understandability.

Surface-based coregistration methods are more redundant than methods based on landmarks; they use the complete structures instead of a limited set of predefined points. An algorithmic overview of surface registration techniques for medical imaging can be found in the article [AFP00]. One popular method with PET brain images is *the hat and head method* [Pel94]. It fits an external surface ”hat” from the anatomical image to the surface ”head” from the functional image by applying the maximum likelihood estimation. The implementation of the method provides convenient interactive control for the registration process [Ero98]. In the past, low computational complexity was also a significant feature. Image coregistration based only on the outer surfaces of the brain might not provide an optimal mapping for the inner structures.

A voxel-based method maps data from one voxel to another voxel. Three widely applied examples applying the voxel classification of brain images are *automated multi-modality image registration* (AMIR), *automated image registration* (AIR), and *statistical parametric mapping* (SPM) methods [ABH$^+$95, WMC93, FAF$^+$95, AF97]. All provide fully-automated coregistration and are applied to registration problems in practice with functional and anatomical images. The evaluation of the SPM and AIR coregistration methods with the PET images can be found in [KAPF97]. Both methods were able to solve the MR to PET coregistration problem for PET images.

With the AMIR method, the head contour is first segmented from the MR image. Then the segmented head volumes are classified using the K-means algorithm [JD88]. The registration is based on assumptions that spatially corresponding PET voxels are expected to have similar values. The variance of the PET voxel values within each connected component is minimized. The method was primarily developed to register MR and PET images, but has successfully been applied to other modalities.

The AIR method uses a cost function for measuring the MR and PET misregistration. The underlying assumptions are the same as with the AMIR method. The aim is to find a transformation matrix which maps all the MR voxels with the

same intensity value to a set of similar PET voxel intensity values.

The SPM coregistration algorithm transforms the MR image into the spatial and intensity space of a representative PET image. The MR image is classified into grey matter, white matter, cerebrospinal fluid and background voxels. Then, the MR image is fitted to an MR template image by using 12-parameter affine transformations. Voxel intensities of grey matter and white matter of the fitted image are modified to correspond to the voxels in the PET image. This image is then mapped to the original PET image.

Inter-subject, intra-modality

The intrinsic methods can be applied to the alignment of studies of different subjects in the same modality. The individual variations need to be mapped to a template image, which may be one image from the set studied or an atlas image. The straight forward way is to remove individual details by smoothing the images before determining the transformation parameters. This could be an appropriate approach for a statistical group studies.

Inter-subject, inter-modality

The last category, alignment of studies of different subjects across different modalities requires advanced methods due to individual variations and differences between modalities. Determination of transformation parameters requires the application of non-linear methods. The registration of functional images can indirectly be done by using the transformation obtained from the anatomical images. A template image or a brain atlas can be used as the link between the images.

3.4 Brain Warping Methods for Non-Linear Image Fusion

Brain warping combines advanced techniques from image segmentation, brain image registration and brain atlases to help the neurological image analysis. It focuses particularly on methods that apply elastic non-linear registration methods

[TT99, Chapter 1]. Three-dimensional elastic methods has been under active study for more than a decade, see for example [BK89]. The aim is to register an individual brain image to some template brain image to allow comparison of brain structures from different individuals (inter-subject). A template brain image may be selected from images studied, or it may be an average image from a representative set of images. A non-linear method is required due to individual variations of brain structures and different properties of imaging modalities. Linear mapping is included in the process. As in image registration, warping methods can be divided into feature-based and voxel-based methods. Whereas voxel-based methods minimize some similarity metrics between images, feature-based methods apply geometrical structures from images. A warping method tries to find a good mapping between structures by modifying them elastically. These elastic transformations for brain images have produced numerous different methods [Tog99]. These methods are applicable to a variety of image mapping problems arising from practice [TT00].

Statistical parametric mapping (SPM) is a widely applied approach based on the registration method, introduced in section 3.3, for non-linear brain mapping and image analysis [AF99]. The underlying idea is to map images to the template image which is an average brain image or atlas. The normalized images are then analysed statistically. The relatively strong smoothing as compared to the resolution of functional images is also likely to remove important details from data. This may affect the quantification of images and prevent quantitative studies with small structures.

Sub-structures of the brain can be considered separately. One interesting possibility for the warping of a cortical structure is to open the individual three-dimensional convolutions to the less individual two-dimensional representation. This way individual convolution is turned on the flat map as in [DvECS99]. The fMRI activation patterns were mapped on the Visible Man atlas [oM03]. This method provides an alternative way to model the cortical structure and to consider elastic brain warping in two dimensions. With PET images, flattening of the cortical structure is a different operation, because the individual cortical convolutions cannot properly be seen in images.

3.5 Databases and Compression of Brain Images

The atlas image and its labelling are not sufficient for an automated brain image processing. A brain database can be applied to organize all the necessary information. A database allows storing original data, images, parameters, additional information, analysing models, atlas, and labelling. This way the amount of redundant information can be minimized and the image retrieval performance optimized. Such a database should be open and distributed to allow full utilisation of the collected data. This could be provided by applying the grid systems [FKT01]. The term *"grid"* refers to an emerging network-based computing infrastructure. It provides security, resource access, information, and other services to control sharing of resources. The resources can be dynamically applied among the individuals and institutions with common interests. In practice, there are many unsolved problems before a global virtual database can be established in the field of medical imaging; to mention a few examples how to protect individual information related to the data, how to cope with the differences between existing imaging systems from different institutes, and how to solve ownership questions of data.

Transmitting images over networks requires compression of image data. A comprehensive overview of compression methods can be found in [GG92]. The properties of PET images (Section 2.3) poses a real challenge for image compression methods and hence application specific methods are usually applied. A lossy dynamic image data compression method for medical images is presented in [HF97]. They use a three-step technique to compress FDG-PET images and a compression ratio greater than 80:1 was achieved. This method was integrated into the database implementation for dynamic PET images [CFF00]. Because the possible future applications of image data are unknown, the lossy compression of data is not advisable with PET brain images. The reliability of quantification may significantly decrease with lossy methods or even vanish. Due to the properties of brain images, the construction of efficient and fast lossless compression is a rather demanding task. The compression method should be fast, because the grid system can distribute the image processing to available facilities in the network. General compression methods designed for one-dimensional signals may not be optimal

for three-dimensional (or four-dimensional) images without modifications. The external knowledge from a target in images should be applied to improve compression ratio and speed. For example, this can be done by first partitioning image data in a suitable way based on the expectations regarding the data. The general compression methods with optimal parameters can then be efficiently applied to these partitions.

Inevitably, a large virtual database raises the question of how efficiently the desired piece of information can be retrieved. A usual way is to use added textual descriptions of the image and its structures. These descriptions are subjective and hence they may have some variations. Moreover, future needs are difficult or even impossible to predict. The contents of an image could provide a better way than mere textual descriptions. With functional images, there are only a few studies concerning the contents of image.

One interesting approach for a content-based functional image retrieval database system (FICBDS) for dynamic PET images is described in the article [CFF00]. The system combines image storage, indexing and compression. The non-textual content of an image is defined as a vector describing the activity concentration at different time points in the image. The retrieval method provides the user with easy access to the images in the database through an given example vector, which can be obtained from an example image. However, the statistical and comparative analysis of PET images is possible with the FICBDS, but not performed.

An earlier attempt at a content-based retrieval system (I^2Cnet) from medical images can be found in the article [OCV96]. The system provides query services through WWW from different servers. The underlying retrieval method is based on extracted regions from images, where the geometrical and textural descriptions are interactively determined. A query can be created by using an example or sketched descriptions. Then the query is compared to the database entries to find the best matches.

3.6 Visualization of Brain Images

Image visualization includes the re-sampling data in the new representation for further processing, displaying, and printing as shown in Figure 3.3. The re-

sampling of matrices requires interpolation of data. The usual methods include the nearest neighbour, linear (bi- and tri-linear with images), spline and sinc-function interpolations. The sinc-function can be defined as follows [Wei03]:

$$\mathrm{sinc(x)} = \begin{cases} 1 & ; \quad x = 0, \\ \frac{\sin(x)}{x} & ; \quad x \neq 0. \end{cases} \tag{3.1}$$

The choice of an interpolation method depends on the application requirements; there is a trade-off between the speed and quality of the final result.

The representation of image data in two dimensions requires interpolation between voxels to achieve a visually satisfactory image. An interpolation method selected wrong implies a possibility for misleading interpretations of an image with visual inspection. In general, two-dimensional representation of three-dimensional medical image data needs special attention, because it is applied to medical decision-making [BK00]. The selection of an appropriate interpolation method depends on properties of an output device which is often a display or a printer. However, visually high quality view may require a computationally expensive interpolation method.

The objective of visualization is to represent image data so that the properties of interest can be seen clearly and less important properties are hidden. This can be achieved by manipulating the colourmap, thresholding voxels, selecting segments and selecting viewpoints. A special colour palette can be mapped to the intensity values to emphasize the desired parts of an image. This method is commonly used in clinical imaging applications. Conventionally, an image is viewed slice by slice from a selected projection. From the three-dimensional image, the projections can be taken from three different angles to give an overview of its content. See Figure 2.5 for an example. Naturally, the viewing angle can freely be selected by applying a proper interpolation method. In emission tomography, the brain scan is tried to make according to the AC-PC line shown in Figure 3.2. The term transaxial slice refers to the image cross-sections that follow this line in a brain image.

From a dynamic functional image sequence an animation can be created to illustrate the change of function. This technique can also be applied to visualize metabolic activity change over a longer time period than just one scan session.

For example, the animation of a disease change in positron emission tomography images is presented in the article [SDT+93]. This way the development of a disease could better be understood and the effects of the given treatment better monitored.

The term *superposition* is used especially when overlaying transaxial slices from two or more images which are coregistered and re-sampled to the same spatial space. The superposition method is widely applied in clinical applications to visualize functional images on structural images. The term is also used when transferring extracted boundaries and surfaces from one image to another.

Recent developments with computer graphics have led to many new possibilities for representing volumetric data such as glass-like surfaces, freely selectable sections, adjustable light sources, stereo views, and virtual reality. For example, virtual reality has been applied for planning and simulation of neurosurgery in [KSTT+00]. However, not many of these have practical applications with PET visualization, but they are certainly topics for further research.

3.7 Summary

Neurological images have been the subject of active research in recent decades. Individually shaped brain structures are not easy targets for applications such as the quantification of functional images. The shape and location of the corresponding functional activity visible in images vary widely between individuals. Therefore, the comparison of images from different subjects requires removing those differences. Also, combining images from different modalities in the same individual is difficult, because of the initial incongruity of the anatomical and functional structures. Advanced methods have been developed to address these problems, to name examples, image fusion, brain warping, brain atlases and databases. Together, these methods provide possibilities to analyse and compare brain images from different individuals and modalities.

Chapter 4

Deformable Models for Delineation of Brain Structures

4.1 Introduction to Deformable Models

A DEFORMABLE model is an object including geometric representation, topology, and evolution rules. The geometric representation describes the shape of the object. The shape has a topology which may differ from the object's topology. The initial geometry is required for the deformable model. The shape of the deformable model can be changed according to the evolution rules. The evolution rules connect the deformable model to data allowing its adaptation to the salient features in an image. The deformable model can be thought as an elastic framework which responds to the applied forces and constraints in a natural way. Hence, it is a well-suited approach for segmentation problems arising from the medical images. The state of the deformable model can be described by force-based or energy-based approaches. The deformable models for delineation of three-dimensional structures and non-rigid motions were introduced in [TWK88, KWT87, MT93]. Since then, they have been widely applied for various problems arising in medical imaging [MT96, PXP99].

Deformable models can be classified into continuous and discrete geometric representations [MDA01]. The continuous representation makes it possible to determine the properties such as surface normals at almost any location on a sur-

face. In practice, a continuous representation needs to be discretised before it can actually be computed. With the discrete model, the geometry is only known at a finite set of points. By establishing connectivity relations for the points, a geometric representation can be defined for the deformable model. The discrete model offers a lower computational complexity and a more compact representation for the surface than the continuous representation, but with decreased accuracy. With sparse functional images, the discrete representation could provide a sufficient description for the image data.

The evolution process can also control other properties than the shape of the deformable model. For example, the resolution of the mesh and connectivity relations may be affected. In the most adaptive approaches the deformable model can be split into many, or several deformable models join to one as described in [MT95]. Highly adaptive methods are particularly useful for extracting unknown objects from images whose noise content is low. However, a highly adaptive deformable model could be difficult to control with noisy and low contrast PET images.

4.2 Discrete Representation of Shapes

The choice of the appropriate representation for a structure depends on image dimensions and the application in which the object is to be used. Requirements for a good representation include size, translation, and rotation invariances. The representation utilized may describe edges, skeleton, voxels or other properties of a segmented object. Representations can be divided into continuous and discrete representations, however, this study concentrates on discrete models which can be applied to present the boundaries of an object.

A set of discrete points is $\mathbf{P} = (\mathbf{p}_1, \mathbf{p}_2, \ldots, \mathbf{p}_m)$, where $\mathbf{p}_i \in \mathbb{R}^n$, $n \in \{2, 3\}$. Their connectivity relations are applied to represent the boundary or surface of a segment. The actual locations of points in an image is determined by a reference point $\mathbf{r} \in \mathbb{R}^n$. Connectivity relations define how the actual boundary is reconstructed from the set of points. A geometric representation is a pair $(\mathbf{P}, \mathbf{r}_P)$. The representation is said to be closed if it limits an area in two dimensions or a volume in three dimensions. Otherwise, it is open.

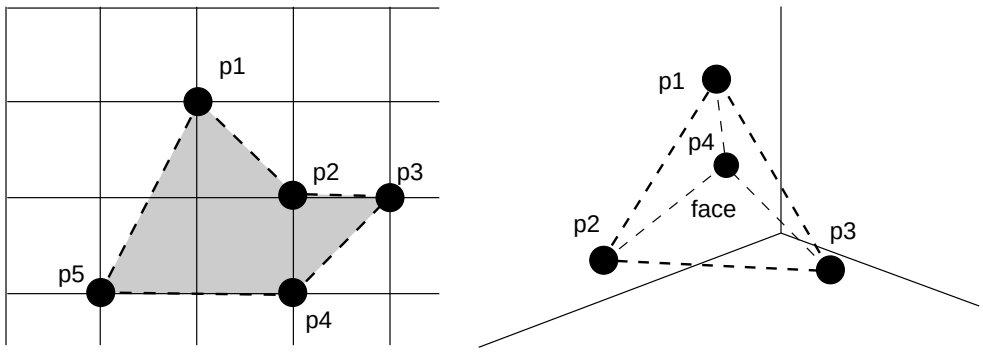

Figure 4.1: A set of connected points (p1-p5) constructs a polygon in two dimensions (a). The points are connected with a broken line (edge) and the area limited is shaded. Triangulated representation of a tetrahedron is shown in (b). A triangular face is defi ned by three points. Four polygons limit the volume.

The polygons defined by a set of points are a simple and computationally efficient method to construct a representation of a curve in a discrete form. A polygon can provide an approximative description for a curve. The connectivity relations can be simply defined by giving the points ($\mathbf{p}_i \in \mathbb{R}^2$) in order to be connected. In the closed curve, the last point ($\mathbf{p}_m$) is connected to the first point ($\mathbf{p}_1$). For example, a polygon limiting a shaded area is visually represented in Figure 4.1 (a).

A three-dimensional object can be represented with a stack of curves. However, coding three-dimensional segmentation this way is not an optimal method. A fixed orientation is especially difficult with three-dimensional rotations. The rotation invariance can be altered.

In three dimensions, points ($\mathbf{p}_i \in \mathbb{R}^3$) with connectivity relations construct a mesh. The mesh is a collection of edges, vertices, and polygons. Each edge is shared by at most two polygons. Connectivity relations can be defined with the aid of neighbouring points. Three points define a triangle which defines a piece of surface, a face [PS85, Chapter 5]. All triangles are selected in such a way that they entirely cover the desired surface. This way three-dimensional surfaces can be represented with a triangulation based on discrete points on a surface. It is

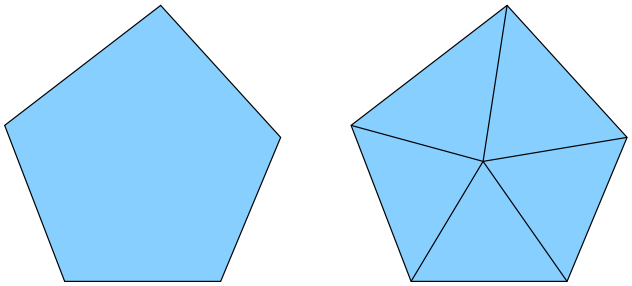

(a) (b)

Figure 4.2: Conversion of a polygon face (a) to the triangulated faces (b).

known as triangulated mesh.

Another possibility is to apply simplex mesh, where the faces are polygons, usually pentagon or hexagon [Del99]. For faces, the mesh points need to be in the same plane, which must be ensured during the construction of the mesh. The simplex mesh is an equivalent representation to the triangulated mesh [PS85, Chapter 5]. For example, a polygon face can be triangulated by setting a new mesh point in the middle of the polygon and creating triangulation as shown in Figure 4.2. However, with the triangulated mesh, more points and their relations need to be stored as compared to the simplex mesh.

The construction of an optimal triangulation from a given segment is a rather difficult task as compared to the construction of curves. For example, the connectivity relations are easy to create for a set of points in two dimensions, but a very complex task in three dimensions. The total number of points, size of triangles, geometry and its topology and the topology of the target to be represented need to be considered to meet the requirements of the application. The surface mesh reconstruction from sample points from the surface of a three-dimensional object is an interesting problem and it has been studied, for example, in [ACK01]. The *power crust method* presented applies the Voronoi diagram and the medial axis transform, which represents an object by the set of maximal balls completely contained in the interiour. Another triangulation method for an arbitrary point set for biomagnetic problems can be found in [LRM98]. It is a modification of the Delanay triangulation.

4.3 Energy of Discrete Deformable Models

The deformation process from the initial geometry to the desired one is often formed as an energy minimization problem. The energy of a deformable model consists of the external and internal energies. While the external energy E_{ext} is determined from an image, the internal energy E_{int} regularizes the geometry of the model. The total energy E of a deformable model is defined as

$$E = \lambda \int E_{int} + (1-\lambda) \int E_{ext}, \tag{4.1}$$

where the regularisation parameter $\lambda \in [0,1]$. Possible external constraints can be added to gain a desired behaviour for the model. With the discrete geometric representation, defined in section 4.2, Equation (4.1) becomes

$$E(\mathbf{P}, \mathbf{r}_P) = \lambda E_{int}(\mathbf{P}) + (1-\lambda) E_{ext}(\mathbf{P}, \mathbf{r}_P) \tag{4.2}$$

$$= \frac{1}{n} \sum_{i=1}^{n} \Big[\lambda E_{int}(\mathbf{p}_i) + (1-\lambda) E_{ext}(\mathbf{p}_i + \mathbf{r}_P) \Big]. \tag{4.3}$$

The objective is to find a minimum for $E(\mathbf{P}, \mathbf{r}_P)$. A local optimization approach is usually applied and hence a fairly good initial geometry is required. The external energy E_{ext} can be defined from an image, for example, by applying the gradient operator (∇f). The gradient image is fixed during the minimization and hence it can be calculated for the image only once. The internal energy E_{int} is bound to the current stage of the model and energy minimization. The internal energy varies during the evolution process.

4.4 Methods for Energy Minimization

Optimization problems can be divided into unconstrained and constrained problems. With unconstrained problems, no limitations are set for the variable values of the solution. Optimization with real world applications, such as energy minimization of a deformable model often requires setting constraints in order to obtain meaningful solutions. The constraints are divided into the soft and hard constraints depending on how restrictive they are. The ultimate aim is to find an optimization method which provides the global solution, is fast, and requires

only little space. Unfortunately, this is not generally possible and hence numerous methods have been developed to meet application requirements.

Optimization methods can be divided into the global and local approaches. Global methods seek the best solution for an objective function. Computationally, finding the exact global solution is often a non-deterministic polynomial (NP) hard problem. This can efficiently prevent the use of the global method for many practical applications where an answer is needed in reasonable time. Therefore, global energy minimization methods have not become popular with three-dimensional deformable surfaces [MDA01]. A local method seeks the best solution by limiting the search. Finding of the global solution cannot be guaranteed. However, if the application specific information can be utilized properly, the global solution for the minimization problem can be found in a reasonable time. Local and global optimization methods can be utilized to seek a minimum for the energy ($E(\mathbf{P}, \mathbf{r}_P)$).

Global Energy Minimization

Dynamic programming was first proposed for the minimization of two-dimensional deformable models in [AWJ90]. It searches globally the minimum energy for the deformable model from the set of all possible solutions. The computational complexity of their method is $O(nm^3)$, where n is the number of points and m is the size of the local neighbourhood to be searched. In three dimensions, the point relations of the mesh cannot be ordered as in two dimensions, leading to computationally expensive algorithms. In theory as well as in practice, dynamic programming leads to unsolvable difficulties with three-dimensional deformable models.

However, the amount of possible solutions can be limited based on the expectations of the object to be searched. One interesting possibility for the global search with deformable curves has been presented in [GN97]. The key idea is to use two curves for the iterative search process instead of one. Two curves are set in a way that the searched object lies in the area between these curves. Initial settings for the dual method are shown in Figure 4.3. The two curves are minimized. Their current energies are compared and the surface having higher

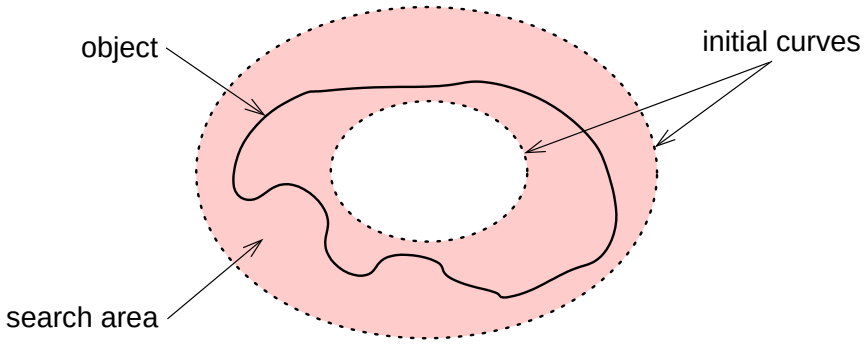

Figure 4.3: Initial settings with the dual curve method [GN97]. The global minimum can iteratively be searched by minimizing two curves.

energy is minimized. When these curves stop in local minima, the curve with the higher energy is minimized with the additional driving force. The driving force pushes the curve towards the other curve until its energy becomes lower. The dual minimization process is continued until the curves become equal. This is the global result of the minimization process.

Local Energy Minimization

In contrast to global approaches, the local optimization has widely been applied with deformable models. A fast search with deformable models can be performed by using, for example, *the greedy method* [WS92]. In principle, the method searches for a minimum for Equation (4.2). In minimization, the greedy method considers only the local neighbourhood, where the best new position for a point is selected. The greedy optimization method requires a appropriate initialization for the deformable model, which is located rather close to the object to be extracted. The time complexity for the greedy method is $O(nm)$, which makes this method more tempting for three-dimensional minimization than dynamic programming approaches. However, the model may be stuck in a strong local minimum and hence the global solution cannot be guaranteed.

4.5 Delineation of Brain Structures with Deformable Models

Delineation of structures from brain images is certainly one important application for deformable models. Deformable models are able to delineate complete structures, adapt individual variances, handle uncontiguous parts in structures and allow the introduction of prior expectations about the structures into the delineation process. These are prerequisites for developing fully automatic approaches for structure extraction from brain images.

However, most of the effort in research has been put into developing structure extraction from anatomical MR brain images. Anatomical structures must be identified for advanced brain mapping, for example. With MR brain images, structure extraction methods are often a collected sequence of operations to produce the final representation of a structure. Pre-processing usually includes removal of unwanted structures from MR images such as the skull tissue from brain images. This is often performed by using manual methods to avoid difficulties later in the delineation process. In the sequence, deformable models are applied to refine the given rough initial surfaces according to the image data. The initial surface for the deformable model may be a generic shape, such as a sphere, or it may be adapted from a given template shape. The deformable model can be used iteratively several times in a processing sequence, where a new initialization can be obtained from the previously extracted surface.

For example, an iterative search to find a parametric representation of the cortical sulci is presented in [VD97]. An elliptic initial surface is first used as the initial surface for the three-dimensional deformable model to extract the outer surface of the brain structure from a pre-processed MR image. Then, the delineated outer surface of the brain is used as the initial surface for the deformable model to obtain the final surface. This kind of iterative approach could also be applied to delineate structures from functional brain images by using a deformable model.

In the literature, there are many newer deformable approaches for the structure delineation from MR images, for example [XPR+99, ZSSD99, MKAE00]. The underlying assumptions for extracting structures from functional images are different than with MR brain images, and these methods could be difficult to apply

to PET brain images. The deformable motion approach to compensate patient motion in gated PET cardiac images was presented in the article [KH02]. However, this problem is rather different than the brain structure extraction problem addressed in this study. In summary, all these studies with MR brain images gave ideas and motivation for delineating surfaces from PET brain images.

Chapter 5

Objectives of the Study

POSITRON emission tomography (PET) imaging provides a way to measure biochemical processes in living organs for drug development and disease diagnosis. PET technique is fairly complicated both technologically and methodologically. The problems are multidisciplinary requiring advanced methodologies for the correct interpretation of acquired data. Comparative and statistical studies in the same modality as well as between modalities with large image sets would be feasible if the regional information could be automatically and reliably collected into a large distributed database. However, this is rather difficult with the present manual or manually guided delineation methods. Noise and low contrast in sparse images together with individual functionality make automatic surface extraction a rather challenging task, particularly in the case of neurological images.

The aim of this study was to investigate lossless image compression and to find and implement a general and automatic procedure for delineating brain surfaces from PET brain images. The complete brain surface should be identified from an image. The segmentation method needed should be able to elastically adapt distinguishable uptake of a radiopharmaceutical in a three-dimensional image. The search should be performed using a global optimization because an initialization close to the object might be difficult to provide for the automatic process. Moreover, the hemispheres of the brain should be automatically separated into left and right to allow separate analysis. If visible in the image, other surfaces should also be delineated for determining structures based on the surfaces.

Chapter 6

Materials and Methods

6.1 Image Material for Evaluations

FUNCTIONAL positron emission tomography studies provided appropriate image material to study surface extraction and compression problems. The noise and low contrast images and the individual variability in the structures of the PET images set the requirements for the methods to be developed. All the image material and calibration information were obtained for the evaluations from the Turku PET Centre [PET03]. The material consists of two phantom studies and a set of selected human studies with ^{18}FDG (fluoro-2-deoxy-D-glucose), FDOPA (fluoro-dopaminium) and ^{11}C-Raclopride radiopharmaceuticals. A phantom is an artificially made object representing the structures of an object. It can be filled with the known volume and activity concentration. The structures in a phantom are static, where there is no blood circulation, natural movements, or changes in substructure volumes as with biological subjects. Hence, it is a useful tool to evaluate new methods developed for neuroimaging. In living human brain studies, the source distribution is unknown.

Sinograms were acquired with ECAT 931/08-12 (CTI/Siemens, Knoxville, TN) and GE Advance (GE, Milwaukee, WI, [MS03]) PET scanners. Transaxial slice width was 6.75 mm with the ECAT scanner and 5.5 mm the GE scanner. The ECAT scanner produces 15 and the GE scanner 35 transaxial slices. The MR images were obtained with 1.5 T Magneton (Siemens, Erlangen, Germany).

The physiological model was calculated into a sinogram using graphical PATLAK [Ale93]. These static sinograms were utilized to reconstruct images for this study. The size of a dynamic sinogram depends on the study and the scanner used.

The images of the striatum phantom were applied to the evaluation in Publication II. The phantom includes the striatum structure of a brain which consists of the caudatus and putamen for both the hemispheres. These structures can be filled with the same radiopharmaceuticals as used in subjects. This setting provides a realistic situation for PET imaging. The images of the Hoffman brain phantom (JB003, Nuclemed N.V./S.A., Roeselare, Belgium) were used for validation in Publication V. The Hoffman brain phantom includes the main structures of the brain. The cross-sections of applied magnetic resonance and positron emission tomography images of the Hoffman phantom are shown on Figure 6.1. The magnetic resonance image was coregistered spatially into the PET image.

The image material from human studies for the publications is summarized in Table 6.1. The MRP reconstructed images acquired with the GE scanner were from the same set of studies in Publications I, III–IV. The images acquired with the ECAT scanner were from the same set in Publications I and II. In addition, corresponding anatomical MR images were used in Publications II and III. The anatomical references were provided only for these ten images. Of the eighteen images, one was found to be miss-aligned after closer inspection and could not be accepted for the final evaluation results.

6.2 Applied Algorithms and Implementations

6.2.1 Image Reconstruction

Two reconstruction methods were available for the study. The conventional FBP method was applied to four human studies in Publication I and to the striatum phantom in Publication II. For this experiment, a Hann filter was chosen for the FBP method. All the other PET images were reconstructed in a standard way with the iterative MRP method (Bayes weight, $\beta = 0.3$) to the size 128×128 [ARA98]. Voxel size in FDOPA and FDG images was $1.72mm \times 1.72mm \times 4.25mm$ and in Raclopride images $2.3mm \times 2.3mm \times 4.25mm$. The Hoffman phantom image

Table 6.1: Image material from PET brain studies of healthy volunteers used with the Publications.

Publication	radiopharmaceutical	scanner	reconstruction	n
I	FDOPA	ECAT	FBP	4
	”	”	MRP	4
	”	GE	”	6
II	FDOPA	ECAT	MRP	5
III	FDG	GE	MRP	4
	FDOPA	”	”	1
IV	FDG	GE	MRP	18
V	FDG	GE	MRP	17
VI	FDG	GE	MRP	17
	Raclopride	”	FBP	4

was reconstructed with an optimal reconstruction zoom by using the MRP method for Publication V. The reconstruction zoom was selected so as to make the brain in the image as large as possible without losing details from the outer surface of the brain.

6.2.2 PET and MR Brain Image Coregistration and Tissue Classification

Three registration methods were available for the study: the hat and head method, the AMIR method and the AIR method [Pel94], [ABH+95, Ero98], [WMC93, Woo03]. Based on initial experiments with the images studied, the corresponding anatomical MR images were coregistered to the PET images with the AMIR method. The MR images were resliced according to the coregistration parameters obtained. The voxels from the MR brain images were classified into grey matter, white matter, cerospinal fluid, and background clusters [JD88]. SPM99 Matlab software was applied for this task [SPM03, MI03]. The classified images were not manually edited. However, the removal of certain structures from the clustered MR brain images is a common procedure after voxel classification.

The coregistration of PET and MR images had two applications in this study. In Publication II, the surfaces extracted from functional PET images were superimposed on the corresponding coregistered anatomical images to check the delineation results. The second use for the registration of PET and MR images was described in Publication III, where the extracted and then coregistered anatomical reference surfaces were superimposed on the corresponding functional PET image to obtain proper initial surfaces. Due to a known error in the applied coregistration program, a fine adjustment of the coregistration was needed.

6.2.3 A New Lossless Compression Method for Emission Tomography Images

Lossless compression is based on redundancy reduction. This can be performed by universal or application specific methods. Because of the relatively low resolution of PET brain images compared to the corresponding anatomical MR images, noise, and individual structures, compression of images requires the application of specific method. In Publication I, we developed a new lossless block method for functional brain images which utilizes local similarity in three dimensions. The method reduces the image variance by subtracting transaxial image cross-sections. The residual image was decomposed into small blocks, which were encoded with a code selected from the parameterized Rice codes [HV93]. However, another predefined library of codes could be used. Algorithms 1 and 2 on page 1242 in Publication I describe the encoding and decoding of an image. The static arithmetic coding was used as a reference method [WNC87]. An overview of the proposed image compression method is given in Figure 6.2.

6.2.4 Delineation of PET Brain Images

Thresholding

A new graphical tool for the delineation of volumetric structures from functional images was developed. Surface delineation from images was based on the thresholding and region growing methods. The surfaces extracted were described as a set of regions, *volume of interest* (VOI), which can be exported as a set of

region of interests (ROI). The structure extraction method is given by algorithms 1 and 2, pages 53-54, in Publication II. The tool provides a framework to make a regional and volumetric analysis from functional emission tomography images. In Publication II, the method was applied to regional quantification from the brain PET images. The striatum structure was studied. The schema of the analysis process is represented in Figure 1, on page 53, in Publication II.

Deformable curves

Two-dimensional deformable models were utilized to search the coarse cortical surfaces in Publication III. We applied the energy-based curve model using the local greedy optimization [WS92]. The implementation was based on the existing software with minor modifications [LC95, Lai95, Lai03]. This software was integrated into the graphical tool introduced in Publication II for the convenient evaluation of the method with PET brain images.

The initial curves for the cortical structure were obtained from the corresponding classified MR images. A set of curves for the brain surface and another set for the white matter surface were delineated by the deformable curve method. The brain surface and the white matter surface are marked in the sketch in Figure 3.1, Chapter 3.1, where these surfaces limit the cortical area. Then, these curves were minimized in the PET image plane by plane with the appropriate parameter values. These included the regularisation λ, two ways to apply λ in energy calculation, see Equations (5) and (6), pages 42 and 43 in Publication III, the size of the local search space for a point and the resolution level of the search. The values were manually selected for each transaxial plane during the delineation of the structure. In addition, the automatic selection of the parameters to extract cortical structure was studied. A set of rules was constructed according to the experiments done for Publication III.

Deformable surfaces

A new three-dimensional deformable model was developed to delineate surfaces from noisy images in [TM03]. Global optimization ensures that the method is not sensitive to its initialization. A preliminary version of the deformable model

applied in this study was featured in [Toh02]. In Publications V, VI and IV, the new deformable model with dual surface minimization (DM-DSM) method was applied to surface delineation from the PET brain images.

The new DM-DSM method combines the desired properties of existing models into a single model. The surfaces are represented as triangulated meshes. Two initial surfaces are iteratively applied to the search process, in principle, as with the dual curve method in [GN97]. The global minimization of the energy allows the use of generic initial surfaces such as an ellipsoid. This is a benefit, because the construction of an optimal mesh for a freely selectable shape is a very complex task.

The surface extraction procedure is presented in Publication VI (section 4, see also Publications V and IV). The ellipsoid was applied as an initial surface for the DM-DSM method for the automatic search of the brain surface. The DSM-OS (DSM - outer surface) variant was applied because energy images usually contain more noise inside the brain volume than outside it. The delineated brain surface was used as an individual initial surface for the search of the white matter surface. The standard DSM algorithm was applied for the white matter surface. Experiments with the ellipsoid and the corresponding white matter surface from the MR image were also conducted.

The DM-DSM method uses the local greedy method to find the energy minimum for the deformable surface in each iteration step [WS92]. With greedy optimization, the surface can be frozen in a local minimum. At an early stage of the study this was avoided by changing the size of the frozen surface. However, this method may cause unwanted movements in those surface parts which are already in the global minimum. Therefore, the energy increase method was introduced in Publication IV, Appendix A. The energy images for the DM-DSM method were computed by the three-dimensional Sobel operator [ZH81]. The preprocessing for FDG-PET and Raclopride images are described in Publication VI (section 4.1).

In addition, the DM-DSM method was applied to the corresponding resliced magnetic resonance images. However, delineation from MR images is a different problem. In this study, it was used to obtain anatomical initial surfaces for functional brain images. The brain surface and the white matter surface were

extracted from the classified MR image by using the DM-DSM method. The extracted brain surfaces from MR and PET images provided an automatic way to adjust the anatomical white matter surface close to the corresponding structure in PET image. The DM-DSM method was used to refine the given initial surface in the PET image.

Iterative structure extraction and quantification

Accurate regional quantification is the aim with functional PET images. To improve the accuracy of regional quantification, the whole process from the sinogram to the quantitative values needs to be considered. The MRP image reconstruction method has excellent noise reduction properties without blurring of the edges of the image. This provided a proper basis for the delineation task and image compression in this study. The quantitative analysis procedure proposed for the FDG-PET brain studies in Publication IV is presented in Figure 6.3[1].

The underlying idea was first to extract structures by identifying the brain surface from the image. Substructures can iteratively be searched starting from the brain surface. The coarse cortical structure based on the brain surface and the white matter surface was extracted using the DM-DSM method. The non-cerebral areas were removed from the structures and quantitative values were determined from these structures.

In Publication VI (section 4.3) the mid-sagittal plane was determined using the delineated brain surface. The symmetry-based algorithm used in this study is very similar to that described in [LCR01]. This method is based on cross-correlations determined from the symmetry of the brain surface.

6.2.5 Visualization of the Delineation

For image visualization, the cross-section views from three different angles were used. The projections of the extracted surfaces were drawn on the images. The

[1]This schema is a part of the poster *"Methods to Improve Repeatability in Quantification of Brain PET Images"* which was presented in the World Congress of Neuroinformatics in Vienna, 2001.

image cross-sections were shown on the screen, usually as grey scale images, and printed on paper as seen on the figures in this study.

With the applied implementation of the two-dimensional deformable curve, the evaluation process can be followed on the screen in real time. This was not possible with the three-dimensional DM-DSM method. To provide easy access to volume rendering and elaborate the evolution process, the intermediate surfaces were exported from the minimization process and transferred into virtual reality modelling language (VRML) format [con03]. The reference surface, the brain surface, was delineated as two volumes of interest with user guided method introduced in Publication II. Two VRML surfaces were created from the hemispheres using the method from [ACK01]. This software was provided for this study as part of a Master's Thesis [Sep01]. A 3D Studio Max script was developed to obtain a three-dimensional volume rendered animation and snapshots from the process [MLIP02, Dis03]. The overview of the visualization process is represented in Figure 6.4[2].

6.3 External and Developed Software Applied

The programs implemented for this study are summarized in Table 6.2. The image analysis programs and some tool programs were provided by Turku PET Centre, and they are summarized in Table 6.3 [Oik03]. Various utilities and software were applied to handle and analyze images during the study. They are summarized in Table 6.4. Parts of the software are available from the Internet, when the address is given in the references. The applied medical image formats are Mayo's Analyze (version 7.5, [Cli03]) and ECAT (version 6.3). The standard formats of the software used were also applied.

[2]This schema is a part of the poster *"Visualization of the Search of Brain Surface in PET"*, which was presented at the IX Turku PET Symposium, Finland, 2002

Table 6.2: Summary of utilities implemented for this study.

Utility	Description	Language
Compression	Image compression tools, Publication I.	C++
ROI programs	Tools to handle ROIs: for finding, combining, splitting, and conversions.	C/C++, gawk
VOI program	A graphical tool for extracting surfaces from images, Publication II and III. The *g-snake* method was integrated in the last version [Lai95].	C/C++
DM-DSM method	Deformable model matlab software, Publications V, VI and IV, [TM03, MI03]	matlab
MS-plane	Determination of the mid-sagittal plane, Publication VI.	matlab
Visualization	A script for 3D Studio Max to create animation from the DM-DSM iteration [MLIP02, Dis03].	3DS Max

Table 6.3: Summary of utilities originating from Turku PET Centre.

Program	Description
amirfit	Automated medical image registration program [Ard95, Ero98].
cti2ana, ana2cti	Image conversion tools from CTI format to the analyse format.
lmhdr, lshdr	Programs to get header information from ECAT format images [Oik03]
patlak	A graphical program to analyse PET images [Ale93].
reslicer	A program to reslice magnetic resonance images from the sagittal to the transaxial orientation. Parameters can be determined, for example, by using the amirfit [Ero98].
roi2kbq	A program to calculate regional quantitative values, current version is named as *img2dft* [Oik03]
surfacefit	The hat and head coregistration program [Ero98, Pel94].
showimg	A simple image and ROI viewer for ECAT format images.

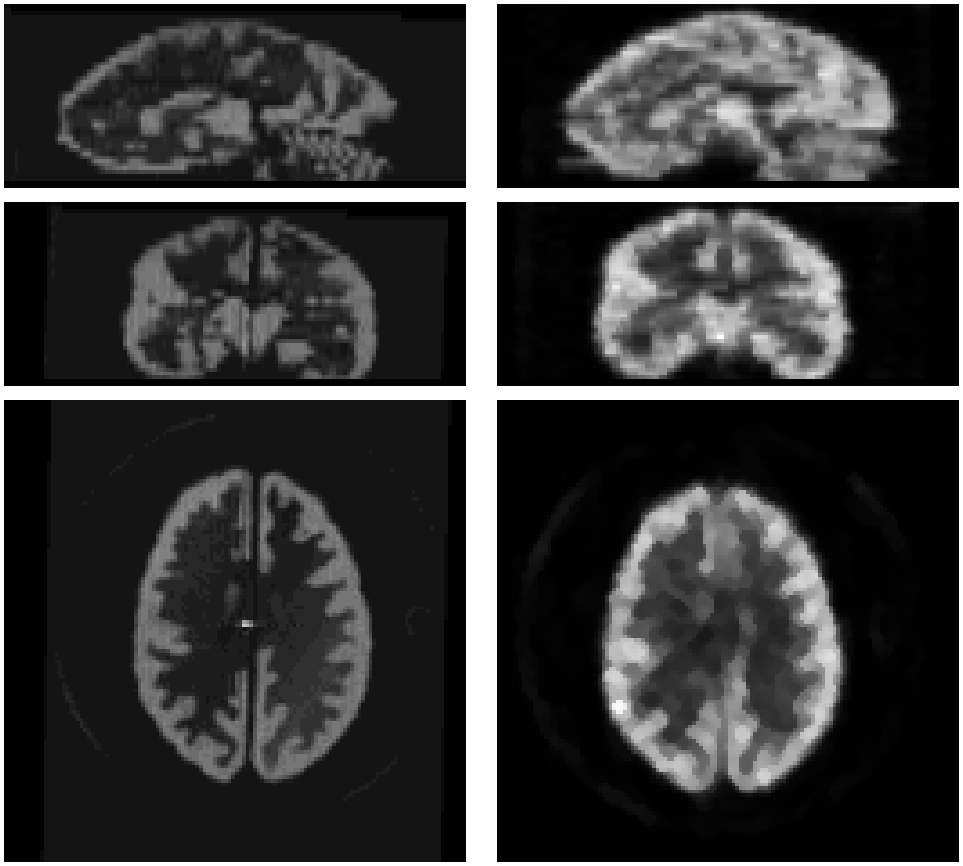

(a) (b)

Figure 6.1: Magnetic resonance (a) and positron emission tomography (b) images of the Hoffman phantom. The MR image is coregistered to the same spatial space as the PET image with the AMIR method [ABH+95]. Top down, sagittal, coronal, and transaxial cross-section views.

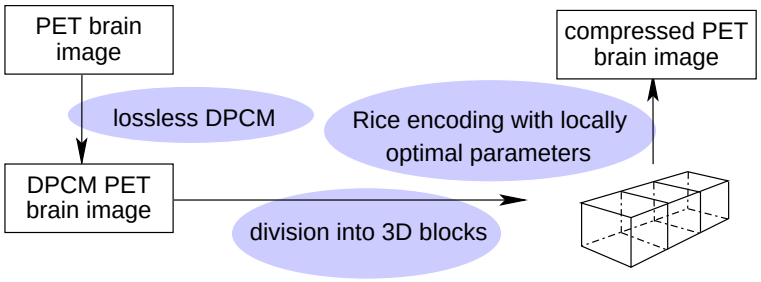

Figure 6.2: Lossless compression of emission tomography images in Publication I. First the differential pulse code modulation (DPCM) was used to form original image. Then the image was divided into volumetric blocks, which were encoded using Rice codes [HV93].

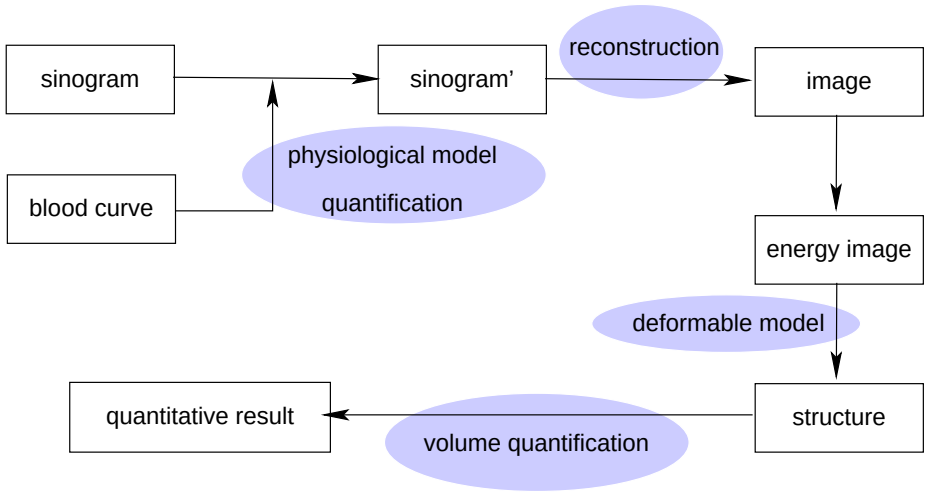

Figure 6.3: Schema of volumetric quantitative analysis of PET brain studies from sinogram to the quantitative result in Publication IV. The physiological model was calculated into a sinogram resulting a static sinogram using graphical PATLAK [Ale93]. This was reconstructed into a three-dimensional image with the MRP method [ARA98]. Surfaces were delineated using the new deformable model as described in Publication V [TM03]. Quantitative regional results were determined from the extracted structures.

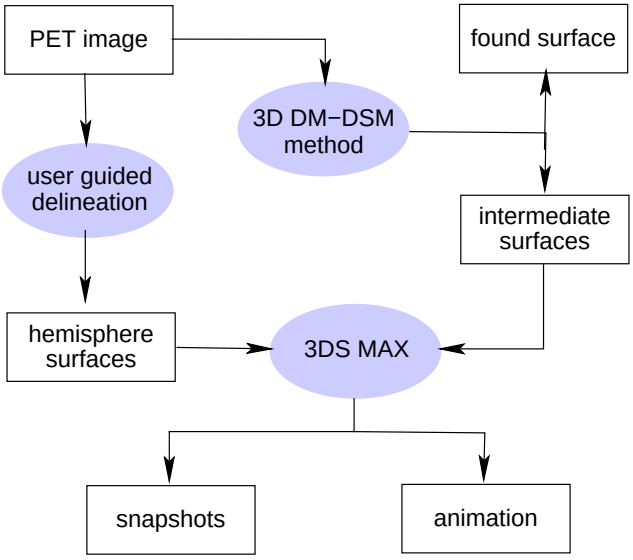

Figure 6.4: Visualization of the search of brain surface in PET [MLIP02]. From the search of the brain surface, the intermediate surfaces were extracted as VRML files. The intermediate surface was the mesh from the current iteration step. The reference surfaces were determined using the user guided method from Publication II. A developed 3D Studio max script created the chosen snapshots and animation for visualization.

Table 6.4: Summary of utilities and software applied in this study.

Utility	Description
AIR	Automated image registration method [WMC93, Woo03].
gsnake	A program for two-dimensional deformable model [Lai95].
imagetool	A program to view and analyse PET and MR images.
powercrust	An algorithm for 3D surface reconstruction [ACK01, ACK03]
SPM96, SPM99	The matlab software for statistical functional image analysis (fMRI, PET). Also includes image classification and registration [SPM03].
Xite	Image processing software for two-dimensional processing [Bøe98]. Capable of handling three-dimensional images as a stacked series of two-dimensional images [xit03].

Chapter 7

Results

THE study is summarized in Figure 7.1 which presents an overview of the topics of this study with related publications. In Publication I the proposed lossless method taking advantage of local similarities of PET brain images was able to improve compression ratio as compared to a plain generic method while keeping the execution time acceptable. The locally adaptive block partitioning method was found better than the basic DPCM method with the arithmetic encoding method. The compressed size of PET images was 40–50% of the original with MRP reconstructed images. The compression ratios for both methods can be found in Table 1, a page 1243 in Publication I. The properties of images produced with the MRP reconstruction method were more favourable for compression than the FBP reconstructed images. It was expected, because of the higher noise level in FBP images.

In Publication II the interactive software developed provided a convenient framework to integrate other software into it and to study these with three-dimensional functional images. With the the thresholding method, it was applied to delineate and to quantify the striatum structure from FDG-PET brain images. Separate threshold values had to be selected for the hemispheres. The method produced the same structures and the same quantitative values in repeated delineations if the initial settings were kept the same. The method was able to reduce the analysis time and the quantitative values determined were comparable to the manual delineation method. The calculated values are presented in Table 1 on page 56 in Publication II. With the applied structure and pharmaceutical matter,

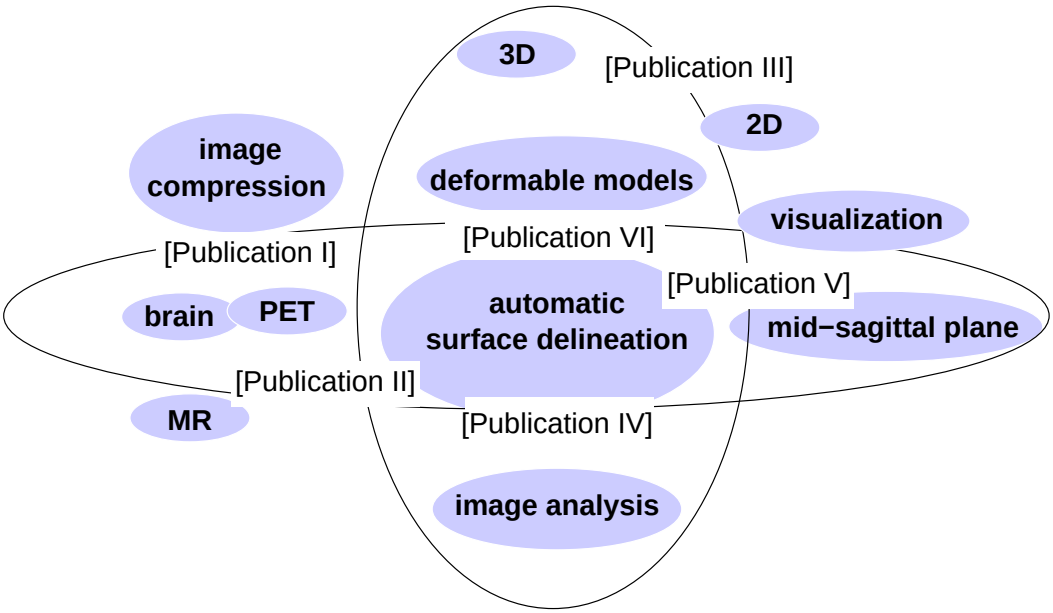

Figure 7.1: Overview of the topics of this study. The publications of this study are positioned near to its main topic.

the thresholding method was appropriate to determine structures. However, in general, this method is applicable only to rather few structures in emission tomography.

In Publication III a general initialization, such as an ellipse, was found too error prone when delineating the brain surface or white matter surface from PET images. The noise and low contrast in the images prevented the use of automatic initialization methods for the curve. Therefore, the initial curves were obtained from the corresponding anatomical structure for the brain surface and the white matter surface. Examples of initial curves are shown in Figures 1-5 overlayed on the corresponding MR (a) and PET (b) image cross-sections, and the minimized curves (c) in Publication III. Deformable curves were able to adapt individual variances present in images which was not possible with the thresholding method without user guidance. The deformable curve method was able to provide acceptable approximations for uncontinuous parts of the edges. It was able to significantly improve the delineated structure compared to the superposition method. With the same initial settings, the method produced the same curves in image

cross-sections. However, many curves still needed manual adjustment and post-editing to obtain a complete three-dimensional structure properly.

In principle, manual adjustment could be replaced by a set of rules guiding structure delineation. These rules were based on knowledge from the structure to be delineated with anatomical initializations. However, these experiments were not successful even with a small set of studied images. The lower areas of the brain structure were particularly difficult in image cross-sections, where they revealed numerous small regions. The fully automatic extraction of three-dimensional structures was found to be a rather hard task using the applied two-dimensional deformable model.

The brain surface was successfully delineated from the studied FDG-PET (Publications IV-VI) and Raclopride brain images (Publication V). Using the extracted brain surface the mid-sagittal planes were determined for all the images (Publication VI). The white matter surface was delineated from all the FDG-PET brain images. Four example snapshots from the brain PET surface extraction process with the DM-DSM method are shown in Figure 7.2 (a)-(d), where the outer surface of the DM-DSM method and the reference surface are shown in images. An example of the extracted mesh of the brain surface and the mid-sagittal plane from one FDG-PET study is presented in Figure 7.3. This mesh and the extracted white matter surface mesh are drawn on the cross-sections of FDG-PET image and energy image in Figure 7.4. An example of the extracted brain surface and mid-sagittal plane for the image from a Raclopride study is presented in Figure 7.5 (Publication VI). The brain surfaces found were excellent for these PET images as well the other studied PET images. The extracted white matter surfaces determined from FDG-PET images were good. The underlying assumptions used for the white matter structure were not as appropriate as for the brain surface and the hemispheres were difficult to describe precisely with a single spherical surface. However, the extracted structure is complete and follows this difficult structure fairly well in the energy image. The coarse cortical structure can automatically be determined from brain PET images based on the brain surface found and the white matter surface. The left cortical and the right cortical volumes of interest were determined for the all FDG-PET brain images in Publication VI.

The delineated brain surface and white matter surface from coregistered MR

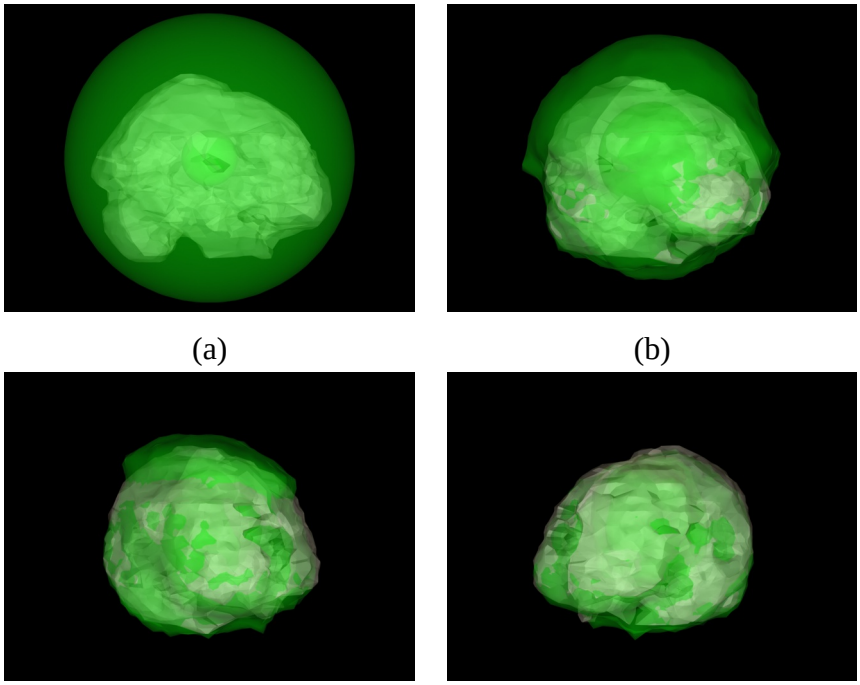

Figure 7.2: Example snapshots from the PET brain surface delineation process with the DM-DSM method [MLIP02]. The reference surface and the outer surface of the DM-DSM method are represented on images: the initial outer surface (a), intermediate states of the outer surface (b) and (c), and the final outer surface. The snapshots were created with the 3D Studio MAX animation software.

images were also good. Examples of extracted surfaces on the MR and the corresponding PET images are shown in Figure 7.6. These surfaces were obtained from the resliced MR images to provide initial surfaces for the experiments in this study. The DM-DSM method could also be a potential method for delineating structures from MR brain images. These experiments with MR images were intentionally omitted from the Publications, because the focus of this study was on functional images.

The general ellipsoid, shown for instance in Figure 7.2 (a), was found to be appropriate initialization for the extraction of the brain surface. It also performed well for the white matter surface. However, the most convenient initialization for the white matter structure was the already extracted brain surface. It was found

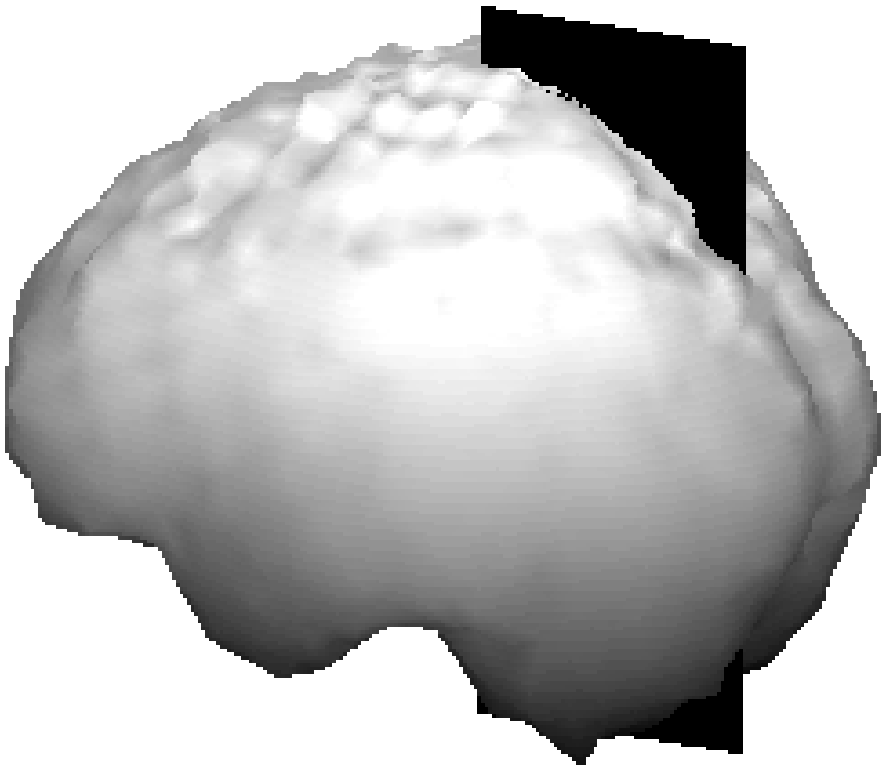

Figure 7.3: Three-dimensional rendering of brain surface mesh extracted from the FDG-PET brain image. The determined mid-sagittal plane is shown on black.

that no corresponding anatomical images were needed in initialization to extract these surfaces, because the DM-DSM method was insensitive to its initialization. Therefore, these results were intentionally omitted from Publications.

The DM-DSM method was resistant to noise with functional PET brain images. It performed the structure delineation in a reasonable time, but not in real time. In practice, with the applied brain surface extraction tasks, the required iterations were usually between 200 and 2000, and at most below ten thousand iterations for a successful search. The applied mesh size was 1280 points. The fewer iterations in the search for white matter than the search of the brain surface was explained by a tighter initialization used with DM-DSM method. With a 200

MHz workstation, the delineation process of a surface takes from few a minutes up to two hours. Figure 7.7 shows the development of the energies of the outer and inner surfaces for the search of the the white matter surface. The outer surface converged fairly fast in the process compared to the inner surface.

In Publication IV the coarse cortical structure was automatically extracted with the DM-DSM method from the 18 MRP reconstructed FDG-PET brain images. On closer inspection of the images, one subject was afterwards found to be misaligned. Hence it was not a relevant image for quantification. With the same initial settings, the DM-DSM method produced the same surfaces. The average influx constants for FDG in the extracted structures were found comparable to the earlier findings with manual methods. The accuracy of regional quantification from functional PET brain images can be improved by using the iterative MRP method for the image reconstruction and the DM-DSM method in an iterative way for the structure delineation.

This study produced new procedures for extracting brain surfaces from volumetric PET brain images based on voxel intensity values. The method introduced in Publications IV–VI is general and automatic approach using the new deformable surface model developed jointly with this study [TM03]. The preceding studies in Publications I–III provided useful methods and knowledge on PET brain images, surface extraction and deformable models to accomplish the task. Brain surface delineation process was the same for FDG-PET and Raclopride PET images, except for pre-processing of images. No anatomical references were needed in the delineation process. The delineated brain surface was used to determine the mid-sagittal plane based on symmetry. Combining these and the white matter surface, the left and right cortical structures from the FDG-PET images were automatically determined.

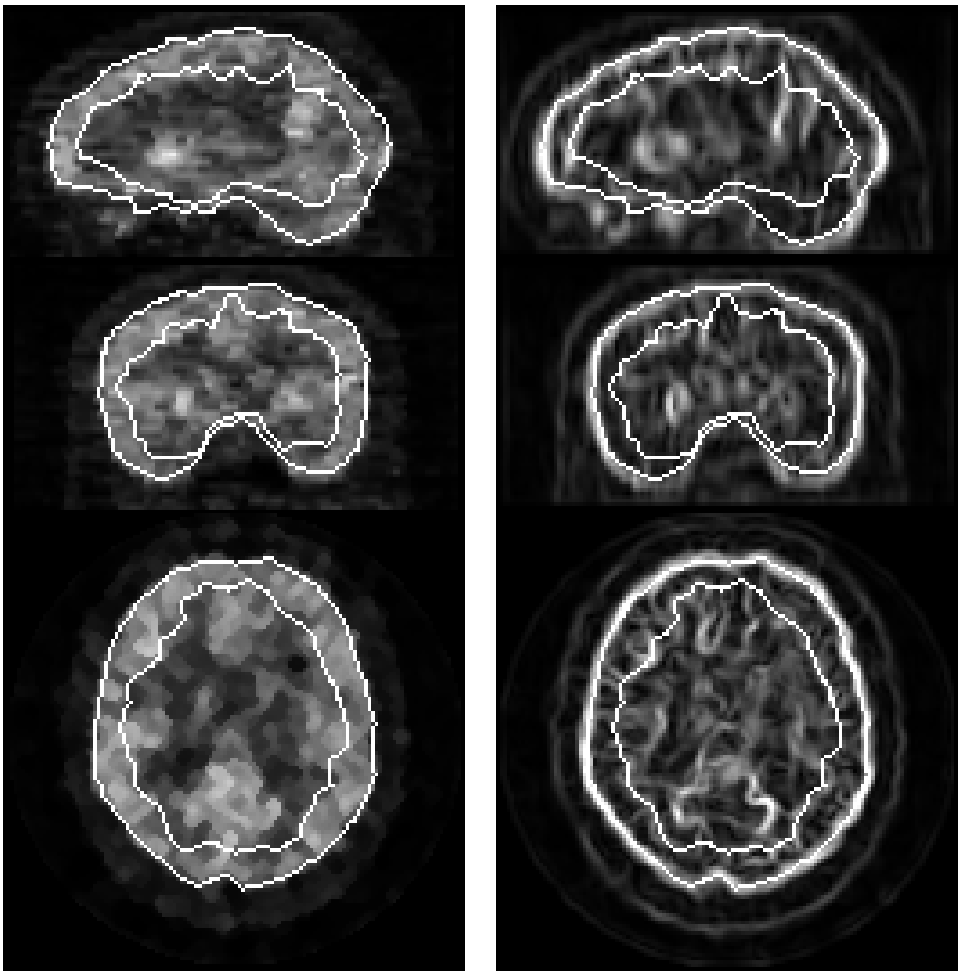

(a) (b)

Figure 7.4: Examples of delineation of cortical structures from one of the human PET brain studies. Projections drawn on the PET image (a) and the energy image (b). From the top, sagittal, coronal and transaxial cross-section views.

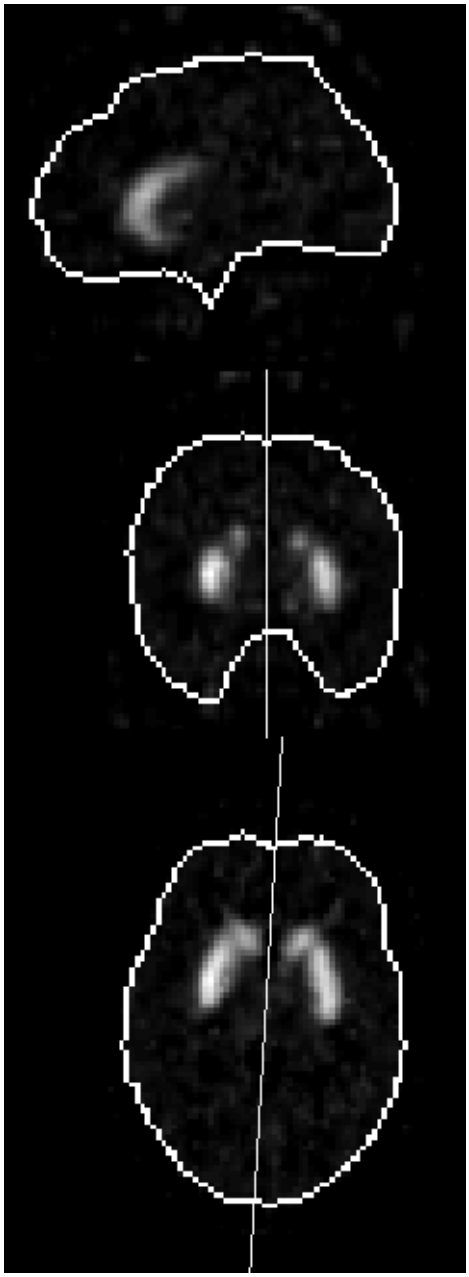

Figure 7.5: Extracted brain surface and mid-sagittal plane from a Raclopride brain image overlayed on the original image.

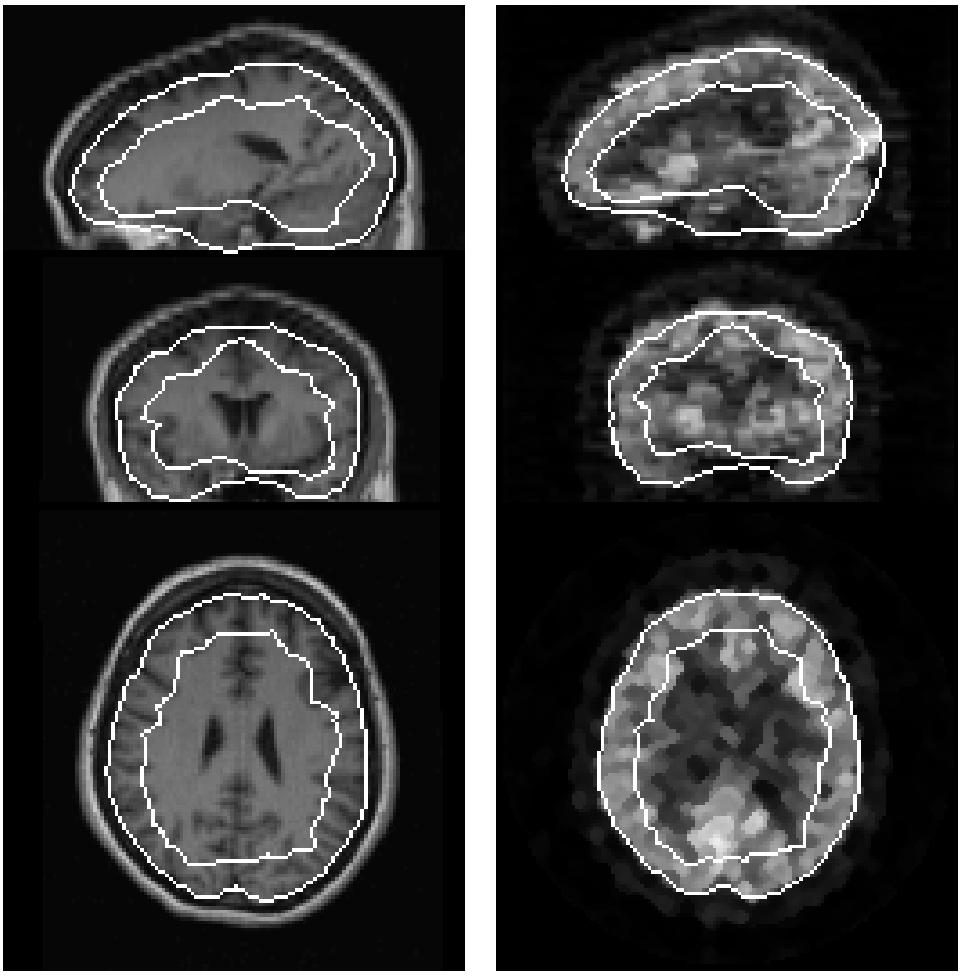

(a) (b)

Figure 7.6: Example of delineation of brain surface and coarse white matter surface from one of the MR brain study. Projections drawn on the MR image (a) and the PET image (b). From top, sagittal, coronal and transaxial cross-section views.

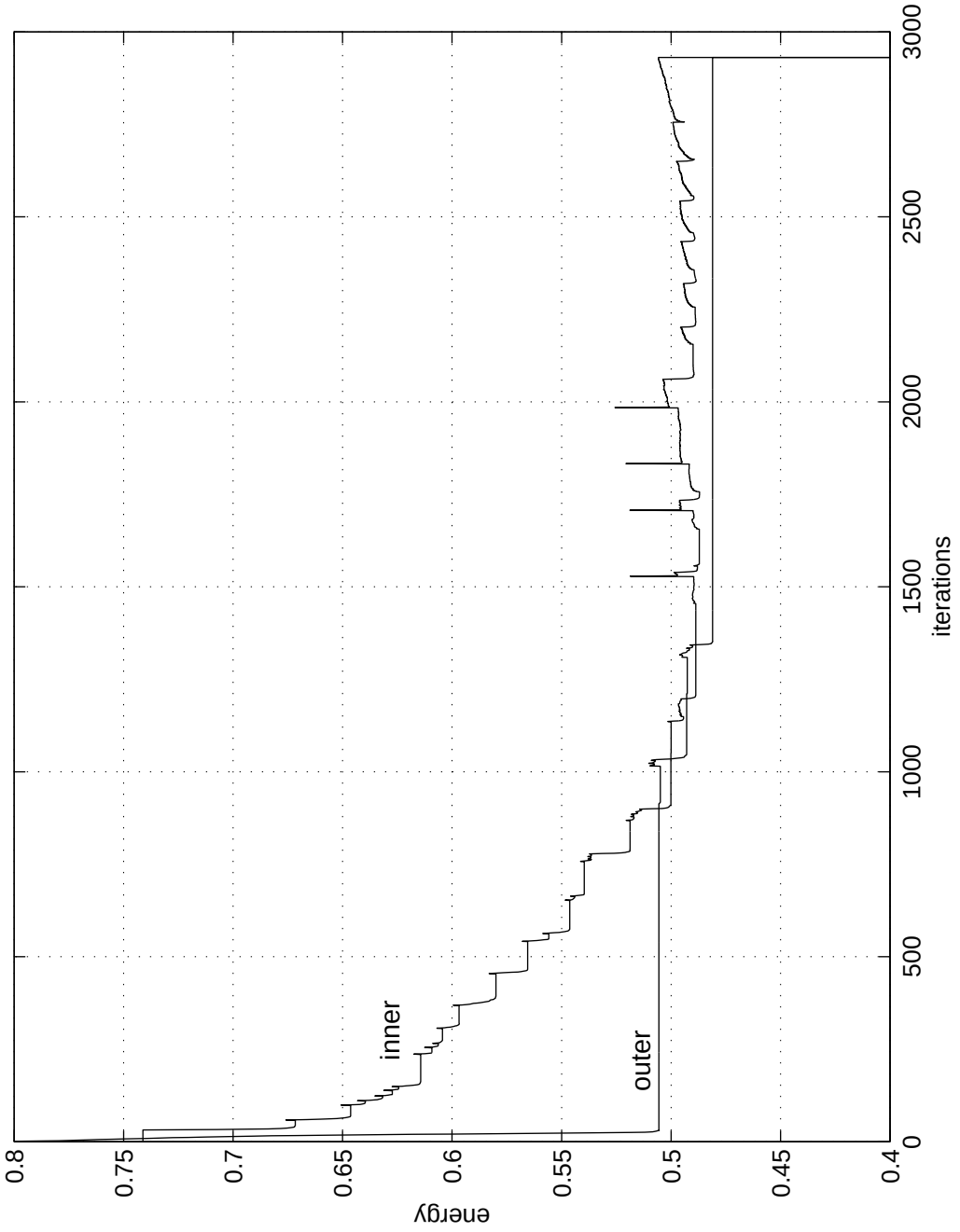

Figure 7.7: Calculated energies of one example search for the outer and inner surfaces during the DM-DSM iterations when searching the white matter surface from the FDG-PET brain image of the phantom. The iterations are stopped when the volume of the inner surface exceeds over the outer surface.

Chapter 8

Discussion

COMPARISON of brain images originating from different subjects is important for neurological studies. This topic was under active research with functional imaging when the current study was started [FGH+97]. The problem is to construct a realignment between two images so that their contents can be compared. Usually images from different individuals are mapped to a common space, for example, Talairach and Tourneux atlas or MNI atlas [Tal88, ECM+93]. Atlases provide a basis for comparative image analysis between subjects, see a work with MR images [GDP+98]. The existing rigid image-to-image mapping methods using affine transformations [PS85, Chapter 1] are appropriate when comparing images originating from the same individual, for example, the surface based method presented in [Pel94]. Between individuals the rigid methods are not able to follow changes in structures and hence they produce inaccuracies for comparisons of images, particularly with PET images. There were attempts at normalizing individual PET images, for example in [ABW+93, FMK+96]. However, these were based on manual processing and did not utilize state-of-the-art image segmentation methods. Elastic methods utilizing content of images are addressed to overcome comparison problems [MRN94]. They apply a non-linear transformation on top of affine transformations.

With PET brain studies, the elastic image mapping methods applied are based on voxel intensity values [WMC93, ABH+95, AF97]. These approaches fullfill many needs in medical image analysis, but not those requiring detailed volumetric information about functions. The intensity values in PET image present the tracer

uptake in a tissue. This depends on the applied radiopharmaceutical and individual changes may be very large. Anatomical structures are not directly visible in PET images, however it is possible to identify many structures, because the function is linked to the anatomy. Visible structures in PET image could be applied as the basis of many applications such as brain mapping. However, poor signal-to-noise ratio and individual variations in the shapes and locations of structures require the use of user guided delineation methods. Automatic methods can be applied, but they usually require hand crafting to obtain acceptable delineation. A histogram of PET images is individual and does not contain clearly distinguishable parts, see Figure 1 in Publication VI. The software applied for delineating regions of interest (ROIs) from transaxial cross-sections of the PET image was the user guided and usually offered thresholding method, see for example in [SDT+93]. The goal of this study became more concrete: to find a general method for segmenting surfaces from PET brain images able to elastically adapt intensity values in an image.

The standard approach to PET image segmentation in image analysis is the superposition method. The externally determined surfaces are overlayed on a PET image for delineating a desired structure. The external surfaces are mainly obtained from the corresponding anatomical MR images, see for example [HKRT98]. The superposition method relies on accurate image registration. With PET images, construction of an accurate registration to the MR images is difficult and it requires a manual method. Obviously, this cannot be a basis for establishing correspondences automatically between images, particularly with large image sets.

The segmentation of only the edges from axial cross-sections of an image does not utilize all the available data from a volumetric PET image. An object present in an image is volumetric and should be considered as a volume limited by its surfaces. Publication II presented an interactive tool for delineating structures from volumetric structures for PET image analysis. A thresholding method was implemented first and it performed well for the image material studied. For a more general approach, the author of this study proposed the use of deformable models for the segmentation of PET images. Deformable models were found to be a useful approach with anatomical images [KWT87, TWK88, MT96]. The energy based two-dimensional deformable model [LC95] was next incorporated into the

tool introduced in Publication III. The aim was to identify the desired properties for the elastic segmentation method because of a lack of existing research with PET brain images. The applied deformable model was able to adapt individual variances present in PET brain images, which is needed for the elastic mapping. Tests showed that a truly three-dimensional deformable model is required for the automatic segmentation of structures from PET images; two-dimensional processing was not able to utilize data from a third dimension. The applied deformable curve model uses a local greedy optimization approach [WS92]. This requires a close initialization, which is difficult to obtain for PET brain structures. With MR brain images there are many possibilities for finding a close initialization, for example the voxel classification, which was applied to creating initialization for the search of cortical structure in [MKAE00, XPR$^+$99]. Unfortunately, most of these are not applicable with PET brain images. Voxels in PET image cannot be classified as with the MR images because voxels depend on the radiopharmaceuticals applied. Hence, energy optimization should be performed globally using the prior information from the object to be delineated. This requirement excluded many promising approaches applied to MR brain images such as topology adaptive deformable models [MT95, MT99].

Without any constraints, global optimization leads to computationally hard problems which are of no use in practical image segmentation problems, such as those considered in this study. For a two-dimensional deformable model the intelligent global search approach was proposed in [GN97]. The idea was to use two deformable curves instead of one. They were initialized in such a way that the searched feature is located between the initializations. Using these two curves, the whole area between these boundaries was globally searched, see more detail in Chapter 4.4.

In this study, two-dimensional deformable models were found insufficient for handling automatic surface delineation from PET brain images. There was clearly a demand for using a three-dimensional method for the segmentation of PET images. However, the existing three-dimensional deformable surface models were not designed for noisy PET images. Therefore, in conjunction with this study, a new three-dimensional deformable surface model was developed [TM03, Toh02]. The global optimization approach and low sensitivity to its initialization allowed

the use of an automatic initialization. For the deformable model, there need to be visible features in an image. For PET images, the pre-processing of images depends on the radiopharmaceutical applied for the study. Two automatic ways of creating energy images for two completely different radiopharmaceuticals, FDG and Raclopride, were presented in this study, see Publication VI. Otherwise, the same parameters were applied to all images for the deformable model, which is a significant benefit over the other segmentation methods designed for a specific application.

The first version of the new three-dimensional deformable surface model was applied in Publication IV and the final version in Publications VI and V. In Publication VI the extracted brain surface was used for automatically determining the mid-sagittal plane from PET brain images. The very good brain surfaces obtained allowed us to apply the existing symmetry based method from [LCR01]. In Publication VI, an automatic and robust segmentation method was found for delineating surfaces from PET brain images. This could have much potential use for automatic brain image analysis. Potential applications, reviewed in Chapter 3, for the automatic brain surface delineation include image compression, image registration, brain warping as well as movement correction.

A standard approach for image compression is to identify redundant (e.g. predictable) data which can be efficiently compressed and the data (e.g. noise) which is difficult to compress. Then, a compression method can be selected to reduce the redundancy. Data classification is an application specific problem and it has been investigated for dynamic PET images, for example in [HF97]. The compression method presented is not lossless limiting the use of compressed image data for the quantitative analysis. This method was integrated into the underlying database framework in [CFF00]. This would allow us to develop the grid system for the storage and computation of neurological imaging [FKT01]. The lossless compression approach introduced for PET brain images in Publication I utilizes local similarities of three-dimensional brain data. This could be improved by applying the extracted brain surface and, for example, compressing the data inside it. Three lossless image compression schemas for medical images were presented in [WN00]. These were applied to two-dimensional images, not including PET images. However, some of the ideas presented could be extended

for three-dimensional images. Newer compression methods could also be applied to PET image compression such as JPEG2000 (Joint Photographic Experts Group) [jpe03].

This study showed that deformable models can be applied to extract brain surfaces automatically from PET brain images for determining the mid-sagittal plane, even from the difficult images from Raclopride studies. In future, these could be applied to develop a new elastic image registration approach needed for the registration of images from different subjects (intra-modality, inter-subject) and especially from different modalities (inter-modality, intra-subject). Existing surface based registration and brain warping methods could also utilize the improved surfaces [Tog99, Chapter 1].

In Publication IV, a principle idea of analysing PET brain image structure by structure was presented. This way extracted structure could be identified and labeled for a more intelligent image analysis. Controlling structures in an intelligent way has also been under investigation for MR images, for example in [LRMK99, MTF+95, MHST02]. Combining structures from anatomical as well as functional brain images is a challenge and has gained increasing interest [BR02]. Delineation of structures from images could be controlled in a global manner using this kind of advanced elastic systems. The surface based delineation procedure introduced in this study provides new aspects for these purposes.

The movement correction from PET brain images would be an interesting application for automatic surface delineation with the new deformable model. The movement correction has earlier been studied with PET cardiac images in [KH02]. An automatic approach handling movements could considerably improve the quality of acquired surfaces from an image sequence. This way, it would affect the accuracy of the quantification of structures. The new deformable model applied in this study could be a useful tool for existing movement correction approaches. A new motion compensation method based on surfaces could also be developed for PET brain images.

This study proposed novel semi-automatic and fully automatic approaches for the surface delineation from functional PET images, and proposed a new lossless image compression approach for PET brain images. The new three-dimensional deformable model using a global optimization was applied to automatic structure

extraction from PET brain images, which was the aim of this study. This opens up new possibilities for developing fully automatic applications for brain image analysis between individuals as well as between modalities.

Chapter 9

Author's Contribution to the Publications

THE work for this study was conducted in close collaboration with the M^{2}oBSI group [Ruo03]. However, the author's contribution to each publication has been essential.

In Publication I a new lossless block method was developed for functional brain images utilizing local similarity in three dimensions. The novelty of the proposed method is that it combines existing ideas applicable to PET brain images. The author of this study participated in the development of the method, performed the experiments and wrote the publication.

Publication II describes the development of a new graphical tool for the delineation and quantification of volumetric structures from functional images. The idea of the tool developed during the author's visit (two months) to Turku PET centre in spring 1997 [PET03]. The author of this study designed the overall principles of the interface, programmed the software, performed the experiments and wrote the publication.

In Publication III the existing two-dimensional deformable model was proposed to search for brain surfaces from PET brain images. The use of deformable models for PET image segmentation was proposed by the author after attending the conference *"Third International Conference on Functional Mapping of the Human Brain"* (Copenhagen, Denmark, 1997) and the course on deformable

models given by D. Metaxas, Ph.D. [FGH+97, TIC97, Met03]. The author of this study participated in the development of the method, integrated the deformable model into the software introduced in Publication II, performed the experiments and wrote the publication.

In Publication IV a new three-dimensional deformable surface model, developed jointly with this study [TM03], was proposed for surface delineation for determining a coarse cortical structure for quantification from FDG-PET brain images. The standard dual surface minimization algorithm was applied for all surfaces. The author contributed the automatic procedure for subsequent surface segmentation to delineate complete structures. The author of this study participated in the development and implementation of the method, and performed the experiments.

In Publication V an improved version of the new deformable model was applied to surface delineation from FDG-PET brain images. The one surface modification of the deformable model was proposed for the search of the brain surface instead of the standard dual surface method. The author of this study performed the experiments and wrote the publication.

In Publication VI the new deformable model was also applied to surface delineation from Raclopride PET brain images. The mid-sagittal plane was determined based on the brain surfaces extracted. The author of this study participated in the design, development of image pre-processing procedure, software integration, the experiments and wrote the main parts of the publication.

Bibliography

[ABH+95] B.A. Ardekani, M. Braun, B.F. Hutton, I. Kanno, and H. Iida. A fully automatic multimodality image registration algorithm. *Journal of Computer Assisted Tomography*, 19(4):615–623, 1995.

[ABW+93] N.M. Alpert, D. Berdichevsky, S. Weise, J. Tang, and S.L. Rauch. Stereotactic transformation of PET scan by nonlinear least squares. In K. Uemura, N. Lassen, T. Jones, and I. Kanno, editors, *Quantification of brain function, tracer kinetics and image analysis in brain PET*. Excerpta Medica, 1993.

[ACK01] N. Amenta, S. Choi, and R. Kolluri. The power crust. In *Sixth ACM Symposium on Solid Modeling and Applications*, pages 249–260, 2001.

[ACK03] N. Amenta, S. Choi, and R. Kolluri. Power curst software. `http://www.cs.utexas.edu/users/amenta/powercrust/welcome.html`, June 2003. (time of checking).

[AF97] J. Ashburner and K.J. Friston. Multimodal image coregistration and partitioning - a unified framework. *NeuroImage*, 6(3):209–217, 1997.

[AF99] J. Ashburner and K.J. Friston. *Spatial normalization*, chapter 2, pages 27–44. In [Tog99], 1999.

[AFP00] M.A. Audette, F.P. Ferrie, and T.M. Peters. An algorithmic overview of surface registration techniques for medical imaging. *Medical Image Analysis*, 4(3):201–217, 2000.

[AHB87] K.S. Arun, T.S. Huang, and S.D. Blostein. Least-squares fitting of two 3-D point sets. *IEEE Transactions on Pattern Analysis and Machine Intelligence*, 9(5):698–700, 1987.

[AKK97] B.A. Ardekani, J. Kershaw, and M. Braun I. Kanno. Automatic detection of the mid-sagittal plane in 3-d brain images. *IEEE Transactions on Medical Imaging*, 16(12):947 954, 1997.

[AKK+99] P.D. Acton, S. Kushner, M-P. Kung, K. Mozley, D. Plössl, and H.F. Fung. Simplified reference region model for the kinetic analysis of $[^{99m}Tc]$ TRODAT-1 binding to dopamine transporters in nonhuman primates using single-photon emission tomography. *European Journal of Nuclear Medicine*, 26(5):518–526, 1999.

[Ale93] S. Alenius. *Patpar program document*. Turku PET Centre, Turku, 1993.

[AR97] S. Alenius and U. Ruotsalainen. Bayesian image reconstruction for emission tomography based on median root prior. *European Journal of Nuclear Medicine*, 24(3):258–265, 1997.

[ARA98] S. Alenius, U. Ruotsalainen, and J. Astola. Using local median as the location of the prior distribution in iterative emission tomography image reconstruction. *IEEE Transactions on Nuclear Science*, 45(6):3097–3105, 1998.

[Ard95] B.A. Ardekani. *Fusion of anatomical and functional images of the brain*. PhD thesis, University of Technology, Sydney, 1995.

[AWJ90] A. Amini, T. Weymouth, and R. Jain. Using dynamic programming for solving variational problems in vision. *IEEE Transactions on Pattern Analysis and Machine Intelligence*, 12(9):855–867, 1990.

[BK89] R. Bajcsy and S. Kovačič. Multiresolution elastic matching. *Computer vision, graphics, and image processing*, 46:1–21, 1989.

[BK00] M. Blank and W.A. Kalender. Medical volume exploration: gaining insights virtually. *European Journal of Radiology*, 33(3):161–169, 2000.

[Bøe98] S. Bøe. XITE, X-based image processing tools and environment, porogrammer's manual, for version 3.4. Technical Report 92, Image Processing Laboratory, Department of Informatics, University of Oslo, 1998.

[BR02] J.F. Brinkley and C. Rosse. Imaging informatics and the human brain project: the role of structure. In R. Haux and C. Kulikowski, editors, *Yearbook of Medical Informatics, Medical Imaging Informatics*, pages 131–148. Schattauer GmbH, 2002.

[Bro92] L.G. Brown. A survey of image registration techniques. *acm computing surveys*, 24(4):325–376, 1992.

[Bro95] J.D. Bronzino. *The biomedical engineering handbook*. CRC, June 1995.

[Bud95] T.F. Budinger. *Instrumentation*, chapter 69.2, pages 1140–1150. In [Bro95], June 1995.

[CFF00] W. Cai, D. Feng, and R. Fulton. Content-based retrieval of dynamic PET functional images. *IEEE Transactions on Information Technology in Biomedicine*, 4(2):152–158, June 2000.

[Cli03] Mayo Clinic. Software: AVW library. `http://www.mayo.edu/bir/Software/AVW/AVWTechInfo.html`, June 2003. (time of checking).

[con03] Web 3D consortium. Vrml. `http://www.vrml.org/`, June 2003. (time of checking).

[Del99] H. Delingette. General object reconstruction based on simplex meshes. *International Journal of Computer Vision*, 32:111–142, 1999.

[Dis03] Discreet. 3d studio max: modeling, animation, and rendering software. `http://www.discreet.com/products/3dsmax/`, June 2003. (time of checking).

[DvECS99] H.A. Drury, D.C. van Essen, M. Corbetta, and A.Z. Snyder. *Surface-Based Analysis of the Human Cerebral Cortex*, chapter 19, pages 337–363. In [Tog99], 1999.

[ECM+93] A.C. Evans, D.L. Collins, S.R. Mills, R.L. Kelly, and T.M. Peters. 3D statistical neuroanatomical models from 305 MRI volumes. In *Proc. IEEE-Nuclear Science Symposium and Medical Imaging Conference*, pages 1813–1817, 1993.

[Ero98] E. Eronen. Lääketieteellisten leikekuvasarjojen kohdistaminen. Licenciate Thesis, Helsinki University of Technology, 1998. In Finnish.

[FAF+95] K.J. Friston, J. Ashburner, C.D. Frith, J-B. Poline, J.D. Heather, and R.S.J. Frackowiak. Spatial registration and normalization of images. In *Human Brain Mapping 2*, pages 165–189. International Conference on Functional Mapping of the Human Brain, New York, Wiley-Liss, 1995.

[FGH+97] L. Friberg, A. Gjedde, S. Holm, N.A. Lassen, and M. Nowak, editors. *Neuroimage, third international conference on functional mapping of the human brain*, volume 5. Academic Press, May 1997.

[FKT01] I. Foster, C. Kesselman, and S. Tuecke. The anatomy of the grid: Enabling scalable virtual organizations. *International Journal of Supercomputer Applications*, 15(3), 2001.

[FMK+96] K.A. Frey, S. Minoshima, R.A. Koeppe, M.R. Kilbourn, K.L. Berger, and D.E. Kuhl. Stereotaxic summation analysis of human cerebral benzodiazepine binding maps. *Journal of Cerebral blood flow and metabolism*, 16(3):409–417, 1996.

[FMR03] FMRIB. Introduction to FMRI, oxford university. `http://www.fmrib.ox.ac.uk/fmri_intro/`, June 2003. (time of checking).

[FvDFH91] J.D. Foley, A. van Dam, S.K. Feiner, and J.F. Hughes. *Computer Graphics, Principles and Practice*. Addison-Wesley, 2nd edition, 1991.

[GDP+98] A.F. Goldszal, C. Davatzikos, M.X.H. Pham, D.L. Yan, R.N. Bryan, and S.M. Resnick. An image processing system for qualitative and quantiative volumetric analysis os brain images. *Journal of Computer Assisted Tomography*, 22(5):827–837, 1998.

[GG92] A. Gersho and R.M. Gray. *Vector quantization and signal compression*. Kluwer Academic Publishers, 1992.

[GLHC97] R.N. Gunn, A.A. Lammertsma, S.P. Hume, and V.J. Cunningham. Parametric imaging of ligand-receptor binding in PET using a simplified reference region model. *Neuroimage*, 6:279–287, 1997.

[GN97] S.R. Gunn and M.S. Nixon. A robust snake implementation: a dual active contour. *IEEE Transactions on Pattern Analysis and Machine Intelligence*, 19(1):63–68, 1997.

[Gra80] H. Gray. *Gray's Anatomy*. Churchill Livingstone, London, 36th edition, 1980.

[HBTL02] B.F. Hutton, M. Braun, L. Thurfjell, and D.Y.H. Lau. Image registration: an essential tool for nuclear medicine. *European Journal of Nuclear Medicine*, 29(4):559–577, January 2002.

[HF97] D. Ho and D. Feng. Dynamic image data compression in spatial and temporal domains: theory and algorithm. *IEEE Transactions on Information Technology in Biomedicine*, 1(4):219–228, Dec 1997.

[HKRT98] R.H. Huesman, G.J. Klein, B.W. Reutter, and X. Teng. Multiscale PET quantitation using three-dimensional volumes of interest. In

R.E. Carson, P. Herscovitch, and M. Daude-Witherspoon, editors, *Quantitative Functional Brain Imaging with Positron Emission Tomography*, chapter 8, pages 51–58. Academic Press, 1998.

[Hor03] J.P. Hornak. The basics of MRI. `http://www.cis.rit.edu/htbooks/mri/`, June 2003. (time of checking).

[HV93] P.G. Howard and J.S. Vitter. Fast and efficient lossless image compression. In J.A. Storer and M. Cohn, editors, *IEEE Computer Society/NASA/CESDIS Data Compression Conference*, pages 351–360, Utah, April 1993. Snowbird.

[ICB03] International consortium for brain mapping. `http://www.loni.ucla.edu/ICBM/`, June 2003. (time of checking).

[Iid02] H. Iida. Tissue heterogeneity – implementation for quantification. In Knuuti and Någren [KN02], page 41.

[JD88] A.K. Jain and R.C. Dubes. *Algorithms for clustering data*. Prentice Hall, 1988.

[jpe03] Jpeg 2000. `http://www.jpeg.org/JPEG2000.html`, June 2003. (time of checking).

[KAPF97] S.J. Kiebel, A. Ashburner, J-B. Poline, and K.J. Friston. MRI and PET coregistration - a crossvalidation of SPM and AIR. *NeuroImage*, 5:271–279, 1997.

[Kar97] P. Karjalainen. *Regularization and Bayesian Methods for Evoked Potential Estimation*. PhD thesis, Kuopio Universtiy Publications C. Natural and Environmental Sciences 61, 1997.

[KH02] G.J. Klein and R.H. Huesman. Four-dimensional processing of deformable cardiac PET data. *Medical Image Analysis*, 6(1):29–46, 2002.

[KIMW00] K. Kneöaurek, M. Ivanovic, J. Machac, and D.A. Weber. Medical image registration. *Europhysics News*, 31(4), Jul/Aug 2000. Available at `http://www.europhysicsnews.com/full/04/article1/article1.html`.

[KN02] J. Knuuti and K. Någren, editors. *Turku PET Symposium*, number D 499 in Annales Universitatis Turkuensis. University of Turku, May 25-28 2002.

[KS01] A.C. Kak and M. Slaney. *Principles of Computerized Tomographic Imaging,*. Society of Industrial and Applied Mathematics, 2001.

[KSTT+00] R.A. Kockro, L. Serra, C. Tseng-Tsai, Y. Chan, S. Yih-Yian, C. Gim-Guan, E. Lee, L.Y. Hoe, N. Hern, and W.L. Nowinski. Planning and simulation of neurosurgery in a virtual reality environment. *Neurosurgery*, 46(1):118–135, 2000.

[KTJ+97] G.J. Klein, X. Teng, W.J. Jagust, J.L. Eberling, A. Acharya, B.W. Reutter, and R.H. Huesman. A methodology for specifying PET VOI's using multimodality techniques. *IEEE Transactions on Medical Imaging*, 16(4):405–415, August 1997.

[KWT87] M. Kass, A. Witkin, and D. Terzopoulos. Snakes: Active contour models. *International Journal of Computer Vision*, 1:321–331, 1987.

[Lai95] K.F. Lai. *GSNAKE API ver 1.0: Reference manual*. Information Technology Institute, 11 Science Park Rd, Singapore 0511, 1995.

[Lai03] K.F. Lai. GSNAKE API, implementation of generalized snake model. `http://www.cs.wisc.edu/computer-vision/projects/gsnake.html`, June 2003. (time of checking).

[LC95] K.F. Lai and R.T. Chin. Deformable contours - modelling and extraction. *IEEE Transactions on Pattern Analysis and Machine Intelligence*, 17(11):1084 – 1090, 1995.

[LCR01] Y. Liu, R.T. Collins, and W.E. Rothfus. Robust midsagittal plane extraction from normal and pathological 3-D neuroradiology images. *IEEE Transactions on Medical Imaging*, 20(3):175–192, 2001.

[LRM98] J. Lötjönen, P-J. Reissman, and I.E. Magnin. A triangulation method of an arbitrary point set for biomagnetic problems. *IEEE Transactions on Magnetics*, 34(4):100–105, Jul 1998.

[LRMK99] J. Lötjönen, P-J. Reissman, I.E. Magnin, and T. Katila. Model extraction from magnetic resonance volume data using the deformable pyramid. *Medical Image Analysis*, 3(4):387–406, 1999.

[MDA01] J. Montagnat, H. Delingette, and N. Ayache. A review of deformable surfaces: topology, geometry and deformation. *Image and Vision Computing*, 19(14):1023–1040, 2001.

[MDB+94] O. Migneco, J. Darcourt, J. Benoliel, F. Martin, Ph. Robert, F. Bussiere-Lapalus, and I. Mena. Computerized localization of brain structures in single photon emission tomography using a proportional anatomical stereotactic atlas. *Computerized Medical Imaging and Graphics*, 18(6):413–422, 1994.

[Met03] D. Metaxas. Home page. `http://www.cis.upenn.edu/~dnm/`, June 2003. (time of checking).

[MHST02] T. McInerney, G. Hamarneh, M. Shenton, and D. Terzopoulos. Deformable organisms for automatic medical image analysis. *Medical Image Analysis*, 6(3):251–266, 2002.

[MI03] The MathWorks Inc. MATLAB: an intuitive language and a technical computing environment. `http://www.mathworks.com`, June 2003. (time of checking).

[MKAE00] D. MacDonald, N. Kabani, D. Avis, and A.C. Evans. Automated 3-D extraction of inner and outer surfaces of cerebral cortex from MRI. *NeuroImage*, 12(3):340–358, 2000.

[MLIP02] J. Mykkänen, J. Luoma, J. Itäranta, and S. Pulkkinen. Visualization of the search of brain surface. In Knuuti and Någren [KN02], page Q05.

[Moh87] N.C. Mohanty. *Signal processing*. Van Nostrand Reinhold, 1987.

[MRN94] M. Moshfeghi, S. Ranganath, and K. Nawyn. Three-dimensional elastic matching of volumes. *IEEE transaction on image processing*, 3(2):128–138, 1994.

[MS03] GE Medical Systems. Functional imaging. `http://www.gemedicalsystems.com/rad/nm_pet/products/pet_sys/advance.html`, June 2003. (time of checking).

[MT93] D. Metaxas and D. Terzopoulos. Shape and nonrigid motion estimation through physics-based synthesis. *IEEE Transactions on Pattern Analysis and Machine Intelligence*, 15(6):580–591, June 1993.

[MT95] T. McInerney and D. Terzopoulos. Topologically adaptable snakes. In *Proceedings of the Fifth International Conference on Computer Vision (ICCV'95)*, pages 840–845. IEEE Computer Society Press, June 1995.

[MT96] T. McInerney and D. Terzopoulos. Deformable models in medical image analysis: a survey. *Medical Image Analysis*, 1(2):91–108, 1996.

[MT99] T. McInerney and D Terzopoulos. Topology adaptive deformable surfaces for medical image volume segmentation. *IEEE Transactions on Medical Imaging*, 18(10):840–850, 1999.

[MTF+95] J.-F. Mangin, F. Tupin, V. Frouin, I. Bloch, R. Rougetet, J. Regis, and J. Lopez-Krahe. Deformable topological models for segmentation of 3D medical images. In *Proc. of Information Processing in Medical Imaging, IPMI95*, pages 153–164, 1995.

[MTF01] J.C. Mazziotta, A.W. Toga, and R.S.J. Frackowiak. *Brain Mapping: The Disorders*. Academic Press, 2001.

[MV98] J.B.A. Maintz and M.A. Viergever. A survey of medical image registration. *Medical Image Analysis*, 2(1):1–36, 1998.

[OCV96] S.C. Orphanoudakis, C.E. Chronaki, and D. Vamvaka. I^2Cnet : content-based similarity search geographically distributed repositories of medical images. *Computerized Medical Imaging and Graphics*, 20(4):193–207, 1996.

[Oik03] V. Oikonen. User guide for programs developed in Turku PET centre, Finland. `http://users.utu.fi/vesaoik/userdocs/`, June 2003. (time of checking).

[oM03] National Library of Medicine. The visible human project. `http://www.nlm.nih.gov/research/visible/visible_human.html`, June 2003. (time of checking).

[Pel94] C.A. Pelizzari. Registration of three-dimensional medical image data. *ICRU News*, pages 4–12, June 1994.

[PET03] Turku PET centre, Finland. `http://www.utu.fi/med/pet/`, June 2003. (time of checking).

[PS85] F. Preparata and M.I. Shamos. *Computational geometry*. Springer, 1985.

[PXP99] D.L. Pham, C. Xu, and J.L. Prince. A survey of current methods in medical image segmentation. Technical Report JHU/ECE 99-01, Depatment of Electrical and Computer Engineering, The Johns Hopkins University, Baltimore MD 21218, 1999.

[Rao78] S.S. Rao. *Optimization, theory and applications*. Wiley Eastern Limited, 1978.

[Ruo97] U. Ruotsalainen. *Quantification and data analysis in positron emission tomography: organ blood flow, graphical analysis and*

radiation dosimetry. PhD thesis, Tampere University of Technology Publications 224, 1997.

[Ruo03] U. Ruotsalainen. Methods and models for biological signals and images M^{2}oBSI. `http://www.cs.tut.fi/sgn/m2obsi/`, June 2003. (time of checking).

[Rus95] J.C. Russ. *The image processing handbook*. CRC Press, 2nd edition, 1995.

[SDT+93] P.G. Spetsieris, V. Dhawan, S. Takikawa, D. Margouleff, and D. Eidelberg. Imaging cerebral function. *IEEE Computer Graphics and Applications*, 13(1):15–26, 1993.

[Sep01] A. Seppälä. Pintoja kuvaavien verkkojen muodostaminen ja optimointi. Master's thesis, University of Tampere, December 2001. In Finnish.

[SPM03] Statistical parametric mapping (SPM), a matlab software for medical image analysis. `http://www.fil.ion.ucl.ac.uk/spm/`, June 2003. (time of checking).

[Tal88] J. Talairach. *Co-planar stereotaxic atlas of the human brain: 3-dimensional proportional system : an approach cerebral imaging / by Jean Talairach and Pierre Tournoux*. Stuttgart: Thieme, 1988.

[TIC97] Tampere International Center for Signal Processing TICSP. TICSP newsletter. `http://sigwww.cs.tut.fi/TICSP/NEWSLETTER/nl_September_97.htm`, Sep 1997.

[TM00] A.W. Toga and J.C. Mazziotta. *Brain Mapping: The systems*. Academic Press, 2000.

[TM03] J. Tohka and J.M. Mykkänen. Deformable mesh for automated surface extraction from noisy images. Accepted for publication in the Special Issue on Deformable models for Image Analysis and Pattern Recognition for *International J. of Image and Graphics*, 2003.

[TMT01] P.M. Thompson, M.S. Mega, and A.W. Toga. *Disease-specific brain atlases*, chapter 6. In [MTF01], 2001. Available at `http://www.loni.ucla.edu/~thompson/PDF/DisChptWeb.pdf`.

[Tog99] A.W. Toga. *Brain Warping*. Academic Press, 1999.

[Toh02] J. Tohka. Surface extraction from volumetric images using deformable meshes: A comparative study. In *Proc. of 7th European Conference on Computer Vision*, number 2352 in Lecture Notes in Computer Science, pages 350 – 364, 2002.

[TT99] A.W. Toga and P. Thompson. *An Introduciton to Brain Warping*, chapter 1, pages 1–26. In Toga [Tog99], 1999.

[TT00] A.W. Toga and P.M. Thompson. *An introduction to maps and atlases of the brain*. In [TM00], 2000. Available at `http://www.loni.ucla.edu/~thompson/PDF/BM2Chpt.pdf`.

[TWK88] D. Terzopoulos, A. Witkin, and M. Kass. Constraints on deformable models: recovering 3D shape and nonrigid motion. *Artificial Intelligence*, 36:91–123, 1988.

[UCL03] School of Medicine UCLA. Let's play pet. `http://www.crump.ucla.edu/software/lpp/l`, June 2003. (time of checking).

[VD97] M. Vaillant and C. Davatzikos. Finding parametric representation of the cortical sulci using an active contour model. *Medical Image Analysis*, 1(4):295–315, 1997.

[Wei03] E.W. Weisstein. Sinc function. Eric Weisstein's World of Mathematics. `http://mathworld.wolfram.com/SincFunction.html`, June 2003. (time of checking).

[WMC93] R.P. Woods, J.C. Mazziotta, and S.R. Cherry. Automated image registration. In K. Uemura, N. Lassen, T. Jones, and I. Kanno, editors, *Quantification of Brain Function, Tracer Kinetics and Image Analysis in Brain PET*, pages 391–398. Excerpta Medica, 1993.

[WN00] J. Wang and G. Naghdy. Three novel lossless image compression schemes for medical image archiving and telemedicine. *TelemedJ*, 6(2):251–260, 2000.

[WNC87] I.H. Witten, R.M. Neal, and J.G. Cleary. Arithmetic coding for data compression. *Communications of the ACM*, 30(6):520–540, Feb 1987.

[Woo03] R. Woods. Automatic image registration. `http://bishopw.loni.ucla.edu/AIR5/`, June 2003. (time of checking).

[WS92] D.J. Williams and M. Shah. A fast algorithm for active contours and curvature estimation. *CVGIP: Image Understanding*, 55(1):14–26, 1992.

[xit03] Xite, x-based image processing tools and environment. `http://www.ifi.uio.no/forskning/grupper/dsb/Software/Xite/`, June 2003. (time of checking). Image Processing Laboratory, Department of Informatics, University of Oslo.

[XPR+99] C. Xu, D.L. Pham, M.E. Rettmann, D.N. Yu, and J.L. Prince. Reconstruction of the human cerebral cortex from magnetic resonance images. *IEEE Transactions on Medical Imaging*, 18(6):467–479, 1999.

[ZH81] S. Zucker and R. Hummel. A three-dimensional edge operator. *IEEE Transactions on Pattern Analysis and Machine Intelligence*, 3(3):324–331, 1981.

[ZSSD99] X. Zeng, L.H. Staib, R.T. Schultz, and J.S. Duncan. Segmentation and measurement of the cortex from 3-D MR images using coupled-surfaces propagation. *IEEE Transactions on Medical Imaging*, 18(10):927–937, 1999.